

Hydrological Response of Andean Catchments to Recent Glacier Mass Loss

3

4 Alexis Caro¹, Thomas Condom¹, Antoine Rabatel¹, Nicolas Champollion¹, Nicolás García²,
5 Freddy Saavedra³

6 ¹ Univ. Grenoble Alpes, CNRS, IRD, INRAE, Grenoble-INP, Institut des Géosciences de l'Environnement,
7 Grenoble, France

8 ² Glaciología y Cambio Climático, Centro de Estudios Científicos (CECs), Valdivia, Chile

9 ³ Departamento de Ciencias Geográficas, Facultad de Ciencias Naturales y Exactas, Universidad de Playa Ancha,
10 Leopoldo Carvallo 270, Playa Ancha, Valparaíso, Chile

11 Correspondence to: Alexis Caro (alexis.caro.paredes@gmail.com)

12

13 **Abstract.** The impacts of the accelerated glacier retreat in recent decades on glacier runoff changes are still
14 unknown in most Andean catchments, increasing uncertainties in estimating water availability. This particularly
15 affects the Outer Tropics and Dry Andes, heavily impacted by prolonged droughts. Current global estimates
16 overlook climatic and morphometric disparities among Andean glaciers, which significantly influence model
17 parameters. Meanwhile, local studies have used different approaches to estimate glacier runoff in a few
18 catchments. Improving 21st-century glacier runoff projections relies on calibrating and validating models using
19 corrected historical climate inputs and calibrated parameters across diverse glaciological zones. Here, we
20 simulate glacier evolution and related runoff changes between the periods 2000-2009 and 2010-2019 across 786
21 Andean catchments (11,282 km² of glacierized area, 11°N-55°S) using the Open Global Glacier Model
22 (OGGM). TerraClimate atmospheric variables were corrected using *in situ* data, getting a mean temperature bias
23 by up to 2.1°C and enhanced monthly precipitation. Glacier mass balance and volume were calibrated, where
24 melt factor and Glen A parameter exhibited significant alignment with varying environmental conditions.
25 Simulation outcomes were validated against *in situ* data in three documented catchments (with a glacierized area
26 > 8%) and monitored glaciers. Our results at the Andes scale reveal an average reduction of 8.3% in glacier
27 volume and a decrease of 2.2% in surface area between the periods 2000-2009 and 2010-2019. Comparing these
28 two periods, glacier and climate variations have led to a 12% increase in mean annual glacier melt (86.5 m³/s)
29 and a decrease in rainfall on glaciers of -2% (-7.6 m³/s) across the Andes, both variables compose the glacier
30 runoff. We confirmed the utility of our corrected regional simulations of glacier runoff contribution at the
31 catchment scale, where our estimations align with previous studies (*e.g.*, Maipo 34°S, Chile), provide new
32 insights on the seasonal glaciers' largest contribution (*e.g.*, La Paz 16°S, Bolivia) and new estimates of glacier
33 runoff contribution (*e.g.*, Baker 47°S, Chile).

34 1 Introduction

35 The largest glacierized area in the southern hemisphere outside the Antarctic ice sheet is found in the Andes
36 (RGI Consortium, 2017; Masiokas et al., 2020). Andean glaciers supply water for roughly 45% of the population
37 in the Andean countries (Devenish and Gianella, 2012) and for ecosystems (Zimmer et al., 2018; Cauvy-Fraunié

38 and Dangles, 2019). Continuous glacier shrinkage has been detected since the late 1970s, with intensification
39 observed over the past two decades (Rabatel et al., 2013; Dussaillant et al., 2019; Masiokas et al., 2020). Glacier
40 volume loss has helped modulate river discharges, mainly in dry seasons (*e.g.*, Baraer et al., 2012; Soruco et al.,
41 2015; Guido et al., 2016; Ayala et al., 2020).

42 Few studies have estimated glacier changes and their effects on hydrology using observation or modeling
43 focused on specific Andean catchments. For instance, the global-scale study by Huss and Hock (2018)
44 comprised 12 Andean catchments (1980-2100). They defined glacier runoff as all the melt water and rainfall
45 coming from the initially glacierized area as given by the Randolph Glacier Inventory version 4.0. and found an
46 increase in glacier runoff in the Tropical and Dry Andes until 2020, but a more contrasted signal in the Wet
47 Andes: no glacier runoff change was observed in some catchments, whereas others showed a reduction or an
48 increase. However, their estimations overlook the diversity in climate conditions and glacier morpho-topography
49 across the Andes and inside large catchments (Caro et al., 2021): such as, latitudinal and/or longitudinal climate
50 variations and glacier characteristics (glacier size, slope and aspect). This affects the simulation results, as they
51 heavily rely on climate inputs and calibrated parameters. For instance, varying temperature lapse rates could
52 result in significant disparities in glacier melt and the determination of solid/liquid precipitation on glaciers
53 (Schuster et al., 2023). Furthermore, the selection of precipitation factor values is also crucial. Based on local
54 studies, the glacier runoff contribution (glacier runoff relative to the total catchment runoff) in the Tropical
55 Andes was estimated to be around 12% and 15% in the Río Santa (9°S) and La Paz (16°S) catchments,
56 respectively (Mark and Seltzer, 2003; Soruco et al., 2015). For the La Paz catchment, Soruco et al. (2015) found
57 no change in the glacier runoff contribution for the period 1997-2006 compared with the longer 1963-2006
58 period. This was attributed to the fact that the glacier surface reduction over the time-period was compensated by
59 their increasingly negative mass balance. In the Dry Andes, the Huasco (29°S), Aconcagua (33°S) and Maipo
60 (34°S) catchments showed a glacier runoff contribution comprised between 3 and 23% for different catchment
61 sizes between 241 and 4843 km² (Gascoïn et al., 2011; Ragetli and Pellicciotti, 2012; Ayala et al., 2020). These
62 catchments had mainly negative glacier mass balances which were slightly interrupted during El Niño episodes
63 (2000-2008 period), thereby reducing glacier runoff. In the Wet Andes, Dussaillant et al. (2012) estimated that
64 some catchments in the Northern Patagonian Icefield are strongly conditioned by glacier melting. In addition,
65 Huss and Hock (2018) did not identify changes in the glacier runoff of the Baker catchment since 1980-2000.
66 However, these studies focused on a restricted number of catchments, employing diverse input data and
67 methodologies over different periods. As such, these local estimations may not be indicative of the broader
68 trends across the entire Andean region. Notably, even neighboring glacierized catchments can exhibit substantial
69 variations in climatic and topographic characteristics (Caro et al., 2021).

70 Nowadays, the availability of global glaciological products such as glacier surface elevation differences and
71 glacier volume estimation (Farinotti et al., 2019; Hugonnet et al., 2021; Millan et al., 2022) allows for large-scale
72 glacio-hydrological simulations with the possibility to accurately calibrate and validate numerical models at the
73 glacier scale. In addition, modeling frameworks such as the Open Global Glacier Model (OGGM, Maussion et
74 al., 2019) have been implemented to simulate the glacier mass balance and glacier dynamics at a global scale.
75 Therefore, OGGM and the glaciological global dataset, in combination with *in situ* meteorological and
76 glaciological measurements, considering the differences of Andean glaciological zones, can be used to quantify
77 the glacier retreat and the related hydrological responses at the catchment scale across the Andes, while taking

78 the related uncertainties into account. Currently, reconstructions of glacier surface mass balance across the Andes
79 (9-52°S) rely on a temperature-index model. Notably, higher mean melt factor values are identified in the
80 Tropical Andes (0.3-0.5 mm h⁻¹ °C⁻¹), compared to the Dry Andes (0.3-0.4 mm h⁻¹ °C⁻¹) and Wet Andes (0.1-0.5
81 mm h⁻¹ °C⁻¹) (e.g., Fukami & Naruse, 1987; Koisumi and Naruse, 1992; Stuefer et al., 1999, 2007; Takeuchi et
82 al., 1995; Rivera, 2004; Sicart et al., 2008; Condom et al., 2011; Caro, 2014; Huss and Hock, 2015; Bravo et al.,
83 2017).

84 Here, using OGGM, we estimate the glacier changes (area and volume) and the consecutive hydrological
85 responses called glacier runoff (which is composed of glacier melt [ice melt and snow melt] and rainfall on
86 glaciers) for 786 catchments across the Andes (11°N-55°S) with a glacierized surface of at least 0.01% for the
87 period 2000-2019. This approach allows us to study the behavior of glaciers across the entire Andes and within
88 specific catchments (for instance those previously studied). Considering the significant hydro-glaciological
89 variations in neighboring catchments and the potential biases within climatic datasets, the air temperature and
90 precipitation data from the TerraClimate dataset (Abatzoglou et al., 2018) were corrected using *in situ* data
91 across the Andes. On the other hand, the simulation procedure considered the calibration of glacier surface mass
92 balance and glacier volume. Both, corrections of climate as well as calibrations (at the glacier scale) were
93 performed considering the climatic and morphometric differences in the Andes, represented through the
94 glaciological zones (Caro et al., 2021). Given that the most important uncertainties in simulating future glacier
95 evolution come, among other factors, from the implementation of the models during the historical period, we
96 validate our simulation and calibration outcomes against observed data from glaciers and catchments.

97 Section 2 presents the data and methods. In Section 3, we describe the glacier changes and hydrological
98 responses at the glaciological zone and catchment scales across the Andes. In Section 4, we discuss our results
99 and the main steps forward compared to previous research.

100 2 Data and methods

101 This section comprises the processed data used as input and during the modeling framework (Figure 1).

102 2.1 Data collection and preprocessing

103 2.1.1 Historical climate data

104 We used two climate datasets: the TerraClimate reanalysis (Climate box in Figure 1) and *in situ* measurements
105 from meteorological stations (*in situ* measurements box in Figure 1). TerraClimate is based on reanalysis data
106 since 1958, with a 4 km grid size at a monthly time scale, and was validated with the Global Historical
107 Climatology Network (temperature, $r = 0.95$, MAE = 0.32°C; precipitation, $r = 0.9$, MEA = 9.1%) (Abatzoglou
108 et al., 2018). The mean temperature was estimated from the maximum and minimum temperature whereas
109 precipitation data is accumulated on a monthly basis. The meteorological records were compiled from Andean
110 organizations and scientific reports (Rabatel et al., 2011; MacDonnell et al., 2013; Schaefer et al., 2017; CECs,
111 2018; Shaw et al., 2020; Hernández et al., 2021; CEAZA, 2022; DGA, 2022; GLACIOCLIM, 2022; IANIGLA,
112 2022; Mateo et al., 2022; Senamhi, 2022). The mean monthly air temperature measurements were taken from 35

113 off-glacier and on-glacier meteorological stations, the latter being rare, located between 9 and 51°S. However, it
114 is important to note that long-term measurements were not available northward of 9°S (the Inner Tropics, IT). To
115 address this, data from stations located in the Outer Tropics (OT) were used as a reference for temperature
116 corrections in this zone, which could affect the performance in the estimation of calibrated parameters such as
117 the melt factor. The location and main properties of the meteorological stations are shown in Supplementary
118 Table S1.

119 2.1.2 Climatic data correction and evaluation

120 For the temperature variable, we first quantified the local vertical annual temperature lapse rates using the *in situ*
121 measurements for 33 sites across the Andes (see Table and Figure S1). Then, the TerraClimate temperature was
122 corrected with these *in situ* records so that they could be used in the simulations (correction box in Figure 1).
123 Last, the corrected TerraClimate temperature was evaluated via a comparison with the 34 *in situ* data (evaluation
124 box in Figure 1). Conversely, the precipitation variable from the TerraClimate reanalysis was scaled using the
125 mass balance measurements for 10 monitored glaciers and was evaluated for 15 glaciers (correction box in
126 Figure 1). Specific data is available in Tables S3, S4 and S5.

127 Vertical temperature lapse rates (temperature LRs) from the *in situ* records were estimated for each glaciological
128 zone across the Andes as per Gao et al. (2012). The temperature LRs are presented in Figure S1. These gradients
129 were applied to correct the raw TerraClimate temperature on the glaciers (rTC_t). The corrected TerraClimate
130 temperature at the mean elevation of glacier (cTC_t) was calculated using the following equation:

131

$$132 \quad cTC_t = rTC_t + \Gamma * \Delta h, \quad (1)$$

133

134 where Γ is the temperature LR estimated here, and Δh is the elevation difference between a glacier elevation and
135 the mean elevation of the TerraClimate grid-cell where the glacier is located.

136 Then, we assessed the cTC_t in meteorological station locations (9°S-51°S) on a monthly scale, paying attention
137 to the monthly variability in temperature as well as to the mean temperature for all the periods with data. The
138 cTC_t monthly mean variability was evaluated using the Pearson correlation coefficient, whereas the mean
139 temperature for the whole period considered the mean difference between cTC_t and the observed temperature
140 (biases).

141 In addition, the total precipitation was scaled (cTC_p) using precipitation factors (Pf) for each glaciological zone
142 across the Andes (see the relationship between solid precipitation and Pf in equation 3). In a second step we
143 discriminate snowfall and rainfall using a linear regression between the temperature thresholds to obtain the
144 solid/liquid precipitation fraction (Maussion et al., 2019). We ran 31 simulations for 18 glaciers with mass
145 balance measurements across the Andes using Pf values between 1 and 4 taking previous studies into account
146 (Masiokas et al., 2016; Burger et al., 2019; Farías-Barahona et al., 2020). Ultimately, 10 glaciers were selected
147 (see Table S3), because their simulated mass balances showed a closer standard deviation in comparison with
148 measurements. The goal was to find the closest simulated mass balance standard deviation ($simSD_{mb}$) in
149 comparison with the measured mass balance standard deviation ($obsSD_{mb}$) using different Pf values (Equation
150 2).

151

152
$$Pf = \{ 1 \leq Pf \leq 4 : simSD_{mb} \approx obsSD_{mb} \}, \quad (2)$$

153

154 A similar methodology was proposed by Marzeion et al. (2012) and Maussion et al. (2019). The results of the
155 closest simulated mass balance standard deviations and associated Pf are presented in Supplementary Table S3.
156 The simulated annual mass balance was evaluated on 15 monitored glaciers using a Pearson correlation
157 coefficient and bias (as the average difference) from simulated mass balance and measured mass balance
158 (evaluation box in Figure 1). In addition, details such as snow/rainfall partitioning are described hereafter and in
159 the model implementation (Section 2.2).

160 2.1.3 Glacier data

161 Glacier inventory

162 We used version 6.0 of the Randolph Glacier Inventory (RGI Consortium, 2017) to extract the characteristics of
163 each glacier, *e.g.*, location, area, glacier front in land or water (glacier inventory box in Figure 1). The RGI v6.0
164 was checked using the national glacier inventories compiled by Caro et al. (2021), filtering every RGI glacier
165 that was not found in the NGI, to obtain a total glacierized surface area of 30,943 km² (filtering 633 km²). The
166 glacier extent in the RGI v6.0 is representative of the early 2000s. The analysis by catchment and glaciological
167 zones is related to the locations and elevation of these glaciers. Overall, 36% of the total glacierized surface area
168 across the Andes is considered. Over 85% of the glacierized surface area in the Dry Andes (18°S-37°S) and 79%
169 in the Tropical Andes (11°N-18°S) are considered, which corresponds to 11% (3,377 km², in 321 catchments) of
170 the total glacierized area of the Andes. For the Wet Andes (37°S-55°S), 29% of the glacierized surface area in
171 the region is considered, which corresponds to 26% (7,905 km², in 465 catchments) of the total glacierized area
172 in the Andes (see the distribution of the catchments in Figure 2a). The simulated glacierized surface area is lower
173 in the Wet Andes due to the filtering out of the numerous calving glaciers found there.

174 Glacier mass balance

175 The mass balance datasets were comprised of the global glacier surface elevation change product of Hugonnet et
176 al. (2021) (calibration box in Figure 1) and *in situ* measurements of the glacier surface mass balance (evaluation
177 box in Figure 1) since 2000 from different institutions (*e.g.*, Marangunic et al., 2021; WGMS, 2021). Hugonnet
178 et al. (2021) product was quantified for each glacier using the OGGM toolbox (Figure 2d). Then, the geodetic
179 mass balance estimates were obtained for every glacier of the RGI v6.0. *In situ* measurements of the glacier
180 surface mass balance are available between 5°N and 55°S (across all Andean regions) at the hydrological year
181 scale (dates vary according to the latitude). However, the Tropical Andes is represented by just two glaciers
182 (Conejeras and Zongo glaciers), producing an underrepresentation in the evaluation of the simulated mass
183 balance in this region. The location and main characteristics of the 18 monitored glaciers are shown in
184 Supplementary Table S4.

185 **Glacier volume**

186 The global glacier ice thickness product of Farinotti et al. (2019) was used to calibrate each glacier of the RGI
187 v6.0 in OGGM (calibration box in Figure 1). Farinotti et al. (2019) pooled the outputs of five different models to
188 determine the distribution of the ice thickness on 215,000 glaciers outside the Greenland and Antarctic ice
189 sheets.

190 **2.1.4 Glaciological zones and catchments**

191 Eleven glaciological zones across the Andes were compiled from Caro et al. (2021) and all glaciers northward of
192 the Outer Tropics were considered as zone number 12, called the Inner Tropics. To identify the glacierized area
193 in each catchment, a spatial intersection was made between the glaciers identified in the filtered RGI v6.0 and
194 the Level 9 HydroSHEDS catchments (Lehner et al., 2006). Then, we considered catchments with a glacierized
195 surface area $\geq 0.01\%$ (max = 62%, mean = 5%, median = 2%). We selected 786 catchments with a surface area
196 between 3,236 and 20 km² across the Andes (11°N-55°S), including 13,179 glaciers with a total surface area of
197 11,282 km² (36% of the total glacierized surface area in the Andes).

198 Calving glaciers (lake- and marine-terminating, 15,444 km²), primarily located in the Northern and Southern
199 Patagonian Icefields and in the Cordillera Darwin, were not considered because the calving process implemented
200 in this version of OGGM (1.5.3) which relies on Hugonnet et al. (2019) data to calibrate the simulated mass
201 balance, could exhibit significant uncertainty when applied to these particular glaciers. In this regard, Zhang et
202 al. (2023) estimated an underestimation of glacier mass loss for lake-terminating glaciers using geodetic
203 methods, accounting for a subaqueous mass loss of $10 \pm 4\%$ in the central Himalaya during the period 2000 to
204 2020. Their findings revealed that the total mass loss for certain glaciers was underestimated by as much as
205 $65 \pm 43\%$. The glaciers that were not simulated for the internal model inconsistencies account for less than 1% of
206 the total glacierized surface area. The other remaining 4,514 km² filtered glacierized surface area corresponds to
207 glacierized catchments that present an increase in glacier volume but a reduction in the glacierized surface area.
208 Only 59 km² was associated with glaciers filtered in the Outer Tropics 1 zone.

209 We selected the La Paz (Soruco et al., 2015), Maipo (Ayala et al., 2020) and Baker (Dussaillant et al., 2012)
210 catchments located in glaciological regions with different climatic and morphometric characteristics (Caro et al.,
211 2021) to evaluate our simulations in terms of glacier changes and glacier runoff contributions over the period
212 2000-2019. In the La Paz and Maipo catchments, previous hydro-glaciological studies have quantified the
213 impact of glacier changes and their hydrological contribution. However, these studies often overlook relevant
214 processes such as variations in precipitation, temperature corrections, and the simulation of glacier dynamics. On
215 the other hand, in the Baker catchment, there are currently no estimations of glacier runoff contributions. These
216 three catchments allow us to make comparisons with our regional simulations at the Andes scale using consistent
217 data (*e.g.*, corrected climate datasets and glacier outlines) and methods (*e.g.*, simulating mass balance, dynamics,
218 and glacier runoff), update previous results, and provide new glacier runoff estimates. For example, it is
219 necessary to understand what occurs during the prolonged dry period in Central Chile and Argentina. In addition,
220 river discharge records were collected from Soruco et al. (2015) and the CAMELS-CL project (Alvarez-Garretton
221 et al., 2018) for Bolivia and Chile, respectively. In Bolivia, we considered the four glacierized head catchments
222 providing water to the La Paz catchment: Tuni-Condoriri, Milluni, Hampaturi and Incachaca (discharge records
223 from 2001 to 2007) with a total surface area of 227 km² and 7.5% of the glacierized surface area (mean elevation

224 of 5,019 m a.s.l.). In Chile, for the Maipo catchment, we compiled records from Río Maipo at the El Manzano
 225 station (catchment id = 5710001; 4839 km²; discharge records from 1990 to 2019) and Río Mapocho at the Los
 226 Almendros catchments (catchment id = 5722002; 638 km²; discharge records from 1990 to 2019) with a
 227 glacierized surface area of 7.5% (mean elevation of 4,259 m a.s.l.). For the Baker catchment, we used the Río
 228 Baker Bajo Ñadis records (catchment id = 11545000; 27403 km²; discharge records from 2004 to 2019),
 229 considering a glacierized surface area of 8.2% (mean elevation of 1,612 m a.s.l.). Note that only the glacier
 230 runoff contribution will be simulated.

231 2.2 OGGM details

232 We ran the OGGM model (Maussion et al., 2019) for each glacier and then the results per catchment were
 233 aggregated for each of the 786 catchments across the Andes (including the three selected test catchments for a
 234 detailed analysis). OGGM is a modular and open-source numerical workflow implemented in Python that
 235 provides pre-processed datasets such as DEMs, glacier hypsometry, glacier flowlines, etc. that can be used to
 236 explicitly simulate glacier mass balance and ice dynamics using calibrated parameter values for each glacier.
 237 Here, we ran OGGM from Level 2, comprising the flowlines and their downstream lines. However, we used a
 238 new baseline climate time series (corrected TerraClimate) as input data. We also calibrated the mass balances and
 239 the bed inversion (ice thickness) that allowed us to obtain hydrological outputs (glacier runoff) (details in
 240 <https://docs.oggm.org/en/v1.4.0/input-data.html>). The spatio-temporal configuration of the model used in this
 241 study is at the glacier scale and at the monthly time step. The simulation results were analyzed at different spatial
 242 scales: by glacierized catchment, glaciological zone, and regionally.

243 The required input data for running the model are as follows: air temperature and precipitation time series, and
 244 glacier outlines and surface topography for specific years. From these input data we computed annual simulated
 245 processes such as the surface mass balance, glacier volume and area, monthly glacier melt (snow and ice) and
 246 rainfall on glaciers (Figure 1). Modeled processes such as the surface mass balance and glacier volume were
 247 calibrated (Table 1 and Figure 2). The calibration procedure of the parameters was applied per glacier to match
 248 the simulated mass balance 2000-2019 to the geodetic mass balance product from Hugonnet et al. (2021). The
 249 simulated glacier volume was calibrated using Farinotti et al. (2019) product at a glaciological zone scale to fit
 250 the Glen A parameter. In other words, the same Glen A parameter was used for each glaciological zone.

251 First, using a glacier outline and topography, OGGM estimates the flow lines and catchments per glacier, and
 252 then the flow lines are calculated using a geometrical algorithm (adapted from Kienholz et al., 2014). Assuming
 253 a bed shape, it estimates the ice thickness based on mass conservation and shallow-ice approximation (Farinotti
 254 et al., 2009; Maussion et al., 2019). After these numerical steps, it is possible to determine the area and volume
 255 per glacier. The mass balance is implemented using a precipitation phase partitioning and a temperature-index
 256 approach (Braun and Renner, 1992; Hock, 2003; Marzeion et al., 2012). The monthly mass balance mb_i at an
 257 elevation z is calculated as follows:

258

$$259 \quad mb_i(z) = TC_{pi}^{snow}(z) * P_f - M_f * \max(cTC_{ti}(z) - T_{melt}, 0), \quad (3)$$

260

261 where TC_{pi}^{snow} is the TerraClimate solid precipitation before being scaled by the precipitation correction factor (262 P_f), M_f is the glacier's temperature melt factor, cTC_{ti} is the monthly corrected TerraClimate temperature. P_f and 263 M_f parameters are related to the snow/ice onset (T_{melt}) and precipitation fraction (T_i^{snow} and T_i^{rain}). Their values 264 are different across the Andes. T_{melt} is the monthly air temperature above which snow/ice melt is assumed to 265 occur (0°C for the Dry and Wet Andes and 2.1°C for the Tropical Andes). T_i^{snow} is calculated as a fraction of the 266 total precipitation (cTC_p) where 100% is obtained if $cTC_{ti} \leq T_i^{snow}$ (0°C for the Dry and Wet Andes and 2.1°C 267 for the Tropical Andes) and 0% if $cTC_{ti} \geq T_i^{rain}$ (2°C for the Dry and Wet Andes and 4.1°C for the Tropical 268 Andes), using a linear regression between these temperature thresholds to obtain the solid/liquid precipitation 269 fraction. Here, M_f was calibrated for each glacier individually using the previously described glacier volume 270 change datasets (Hugonnet et al., 2021). The calibrated parameter values are summarized by glaciological zone 271 in Table 1.

272

Table 1. Calibrated parameter values used in the glacier mass balance and volume simulations across the Andes (11°N-55°S) during the period 2000-2019

Region	Zone	Mass balance parameter values						Volume parameter
		Temperature LR [°C/m]	Precipitation factor [-]	Mean melt factor [mm mth ⁻¹ °C ⁻¹]	Temperature for melt onset [°C]	Temperature at start of snowfall [°C]	Temperature at start of rainfall [°C]	Glen A inversion [s ⁻¹ Pa ⁻³]
Tropical Andes	IT*	-0.0066	1	434	2.1	2.1	4.1	2.4 10 ⁻²³
	OT2*			284				6.3 10 ⁻²⁴
	OT3*			432				1.2 10 ⁻²³
Dry Andes	DA1	-0.0082	2.8	418				2.4 10 ⁻²⁵
	DA2	-0.0065	1.9	479				1.3 10 ⁻²³
	DA3	-0.0063	4	299				2 10 ⁻²⁴
Wet Andes	WA1	-0.0051	4	103	0	0	2	1.7 10 ⁻²³
	WA2		4	118				1.9 10 ⁻²³
	WA3	-0.0063	2.3	152				6 10 ⁻²⁴
	WA4			128				1.3 10 ⁻²³
	WA5			179				1 10 ⁻²³
	WA6			139				1.5 10 ⁻²³

*related to zones of the Tropical Andes region: Inner Tropics (IT) and Outer Tropics (OT2 and OT3)

273

274 2.2.1 Model setup, calibration and validation

275 The input data are as follows: the corrected monthly TerraClimate precipitation (cTC_p) and temperature (cTC_t), 276 glacier outlines were obtained from RGI v6.0 (RGI Consortium, 2017), assuming the glacier outlines of all 277 glaciers were made for the year 2000. The surface topography data were sourced from NASADEM (Crippen et

278 al., 2016). NASADEM has a spatial resolution of 1 arcsecond (~30m), and the data were acquired in February
 279 2000 (NASA JPL, 2020). The simulated glacier volume was calibrated using Farinotti et al. (2019) product at a
 280 glaciological zone scale to fit the Glen A parameter (Table 1 and Figure 2).

281 Last, the simulated mass balance was evaluated in comparison with *in situ* mass balance observations
 282 (Marangunic et al., 2021; WGMS, 2021). Although the OGGM outputs are in calendar years and the
 283 observations are in hydrological years, we consider it essential to evaluate the interannual performance (Pearson
 284 correlation, p-value, variance, RMSE and bias from average difference) and the cumulative mass balance since
 285 the year 2000.

286

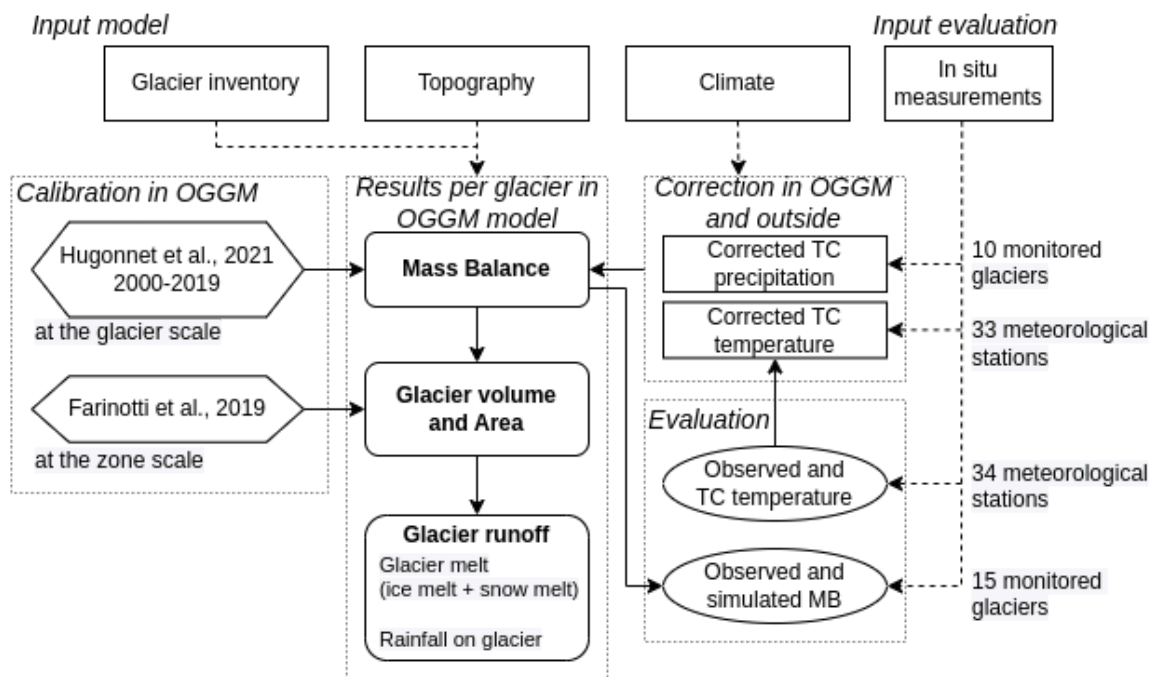


Figure 1. Workflow per simulated glacier using OGGM between 2000 and 2019. Two groups of input data were used: one to run OGGM and the second to correct/evaluate the TerraClimate temperature (cTCt) and precipitation (cTCp). Then, the mass balance and glacier volume were calibrated. Lastly, results such as the cTCt and glacier mass balance were evaluated at 34 meteorological stations and on 15 glaciers with mass balance observations. The corrections in OGGM and outside box refer to analyses performed by running the model and also analyzing data outside the model tool. An example is the estimation of temperature lapse rates, which were estimated from *in situ* measurements but introduced in the OGGM model as a parameter value.

287 3 Results

288 3.1 Climatic variations on glaciers across the Andes during the period 2000-2019

289 The climate associated with 786 Andean glacierized catchments (11°N-55°S) presents a mean corrected
 290 TerraClimate temperature (cTCt) of $-0.2 \pm 2.2^\circ\text{C}$ and a mean annual corrected TerraClimate precipitation (cTCp)
 291 of $2699 \pm 2006 \text{ mm yr}^{-1}$ between 2000 and 2019. The various glaciological regions show significant climatic
 292 differences, with contrasting extreme values between the Tropical Andes and Wet Andes in terms of mean
 293 annual precipitation ($939 \pm 261 \text{ mm yr}^{-1}$ and $3751 \pm 1860 \text{ mm yr}^{-1}$, respectively) and mean annual temperature
 294 between the Dry Andes and Tropical Andes ($-3.7 \pm 1.4^\circ\text{C}$ and $1.3 \pm 0.8^\circ\text{C}$, respectively). Certain glaciological

295 zones highlight very negative and positive mean annual temperature values such as Dry Andes 2 (-4.8°C) and
296 Wet Andes 2 (1.9°C) and lower and higher cumulative precipitation values such as Dry Andes 1 (447 mm yr⁻¹)
297 and Wet Andes 5 (6075 mm yr⁻¹). Meanwhile, variations in climate between the periods 2000-2009 and
298 2010-2019 across the Andes show a cumulative precipitation decrease in -9% (-234 mm yr⁻¹) and a mean annual
299 temperature increase in $0.4 \pm 0.1^\circ\text{C}$. Between these two periods, precipitation is decreasing primarily in the Dry
300 Andes (-256 mm yr⁻¹; -23%) and Wet Andes (-337 mm yr⁻¹; -9%), and increasing in the Tropical Andes (44 mm
301 yr⁻¹; 5%), whereas the temperature is increasing between 0.3-0.4°C in all regions. At the glaciological zone scale,
302 only the Tropical Andes and Dry Andes 1 (12%) show a cumulative increase in precipitation, whereas a larger
303 decrease in precipitation is found in Dry Andes 2 (-32%) and Dry Andes 3 (-27%). The mean annual
304 temperature increases in all zones, especially the Inner Tropics (+0.6°C) followed by Wet Andes 3 (+0.5°C). A
305 summary of variations in climate by glaciological zone is presented in Table 2.

306 Our cTCt evaluation is statistically significant (p-value < 0.01) at 32 meteorological stations with a mean
307 temperature bias of 0.4°C and a mean correlation of 0.96 (These results are available in Table S2 and Figure S2).
308 The regional results show a larger bias in the Tropical Andes (mean = 2.1°C, four stations) with a meteorological
309 station mean elevation of 4,985 m a.s.l., where cTCt cannot represent the mean monthly temperature. However,
310 cTCt well represents the maximum temperatures in spring/summer and the minimum temperatures in winter. The
311 lowest bias is observed in the Wet Andes and Dry Andes. The Wet Andes, with a meteorological station mean
312 elevation of 813 m a.s.l., shows good results in terms of reproducing the mean monthly temperature in most
313 stations, with a minimum correlation higher than 0.86. In the Dry Andes, with a meteorological station mean
314 elevation of 3,753 m a.s.l. (18 stations) and bias of 0.2°C, the cTCt reproduces the mean monthly temperature
315 very well. However, in some stations such as La Frontera and Estrecho Glacier (29°S), the mean cTCt is warmer
316 than 6°C, whereas in other stations such as El Yeso Embalse (33.7°S) and Cipreses glacier (34.5°S), the mean
317 cTCt is colder than 6°C. The detailed cTCt evaluation based on bias and Pearson's correlation can be found in
318 Tables S1 and S3 and Figure S2 of the Supplementary Materials. The cTCt presented a mean bias of 2.1°C in the
319 Tropical Andes and a mean bias of 0.2°C in the Dry Andes and Wet Andes in comparison with *in situ*
320 measurements.

321 3.2 Glaciological changes across the Andes during the period 2000-2019

322 The 36% of the total glacierized surface area across the Andes (11°N-55°S) are simulated to obtain annual
323 glacier area and glacier volume, as well as the monthly glacier runoff (glacier melting and rainfall on glaciers).
324 Considering mean values for the periods 2000-2009 and 2010-2019, the glacier volume and surface area in the
325 Andean catchments show a decrease by -8.3% (-59.1 km³) and -2.2% (-245 km²), respectively. This corresponds
326 to a mean annual mass balance difference between the two periods of $-0.5 \pm 0.3 \text{ m w.e. yr}^{-1}$ (Figure 2d). A
327 decrease in glacier volume and surface is seen in 93% of the catchments (n = 724) whereas 7% of the catchments
328 (n = 65) present an increase in glacier volume and surface. The loss in glacier volume (Figure 2b) is largest
329 (-47.8 km³, -9%) in the Wet Andes, followed by the Tropical Andes (-5.9 km³, -7%) and Dry Andes (-5.4 km³,
330 -6%). Similarly, a larger decrease in the glacier surface area (Figure 2c) is observed in the Wet Andes (-144.4
331 km², -2%), followed by the Tropical Andes (-55.5 km², -4%) and lastly the Dry Andes (-45.2 km², -3%). As
332 expected, the correlation between both glacier change variables is consistent at the zone scale, showing a
333 positive correlation between the changes in area and volume (r = 0.9).

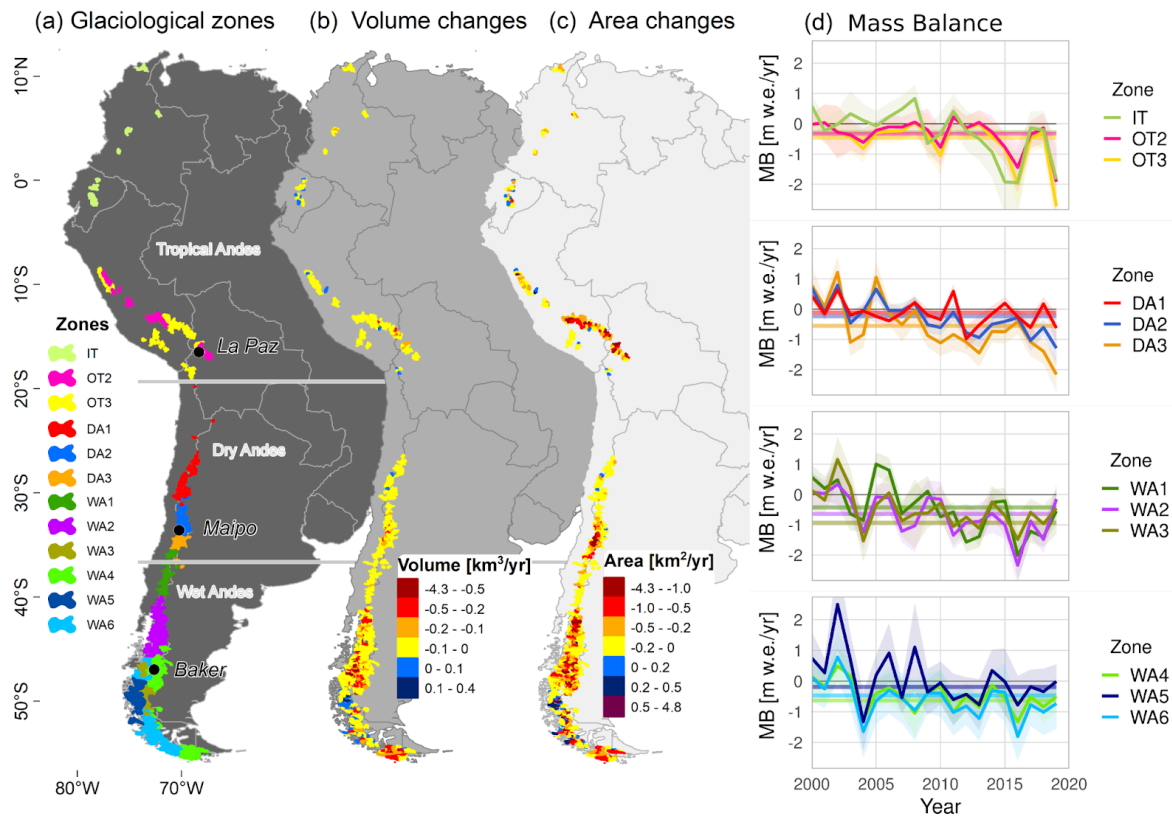


Figure 2. Recent glacier changes across the Andes. The glacier changes represent the mean annual differences between the periods 2000-2009 and 2010-2019 per catchment ($n = 786$). (a) It shows the distribution of the glaciological zones (11°N-55°S), followed by the (b) volume and (c) area changes at the catchment scale. The (d) annual specific mass balances are presented in each glaciological zone (the shaded areas are the standard deviation), where the straight lines correspond to the mean geodetic mass balance (2000-2019) estimated by Hugonnet et al. (2021).

335

336 When estimating the mass balance, it is interesting to check the calibrated melt factors (M_f) of the temperature
 337 index-model in order to evaluate its possible regionalization, i.e. to evaluate the spatial coherence (see Table 1
 338 and Figure 3). The mean calibrated melt factor values decrease from the Tropical Andes toward the Wet Andes
 339 (Tropical Andes = $0.5 \pm 0.3 \text{ mm h}^{-1} \text{ }^\circ\text{C}^{-1}$, Dry Andes = $0.6 \pm 0.2 \text{ mm h}^{-1} \text{ }^\circ\text{C}^{-1}$, Wet Andes = $0.2 \pm 0.1 \text{ mm h}^{-1} \text{ }^\circ\text{C}^{-1}$).
 340 The lowest mean temperatures estimated in the Dry Andes imply higher factor values to reach the calibrated
 341 mass loss in the few months in which the temperatures exceed 0°C . The opposite can be observed in the Wet
 342 Andes, where low factor values are associated with a greater number of months with temperatures exceeding
 343 0°C . We obtain very similar values in contiguous zones, with the lowest values found in the Wet Andes (mean
 344 below $179 \text{ mm mth}^{-1} \text{ }^\circ\text{C}^{-1}$), followed by the Tropical Andes (mean below $434 \text{ mm mth}^{-1} \text{ }^\circ\text{C}^{-1}$), and the Dry Andes
 345 (mean below $479 \text{ mm mth}^{-1} \text{ }^\circ\text{C}^{-1}$). The largest melt factor values are found in the Dry Andes where the Dry
 346 Andes 2 zone (mean = $479 \text{ mm mth}^{-1} \text{ }^\circ\text{C}^{-1}$) presents the lowest mean temperatures across the Andes (-4.8°C
 347 between 2000-2019). The lowest melting factor values are calibrated in the Wet Andes where zone Wet Andes 1
 348 (mean = $103 \text{ mm mth}^{-1} \text{ }^\circ\text{C}^{-1}$) shows high mean temperatures (1.8°C between 2000-2019). Despite this, a lower
 349 correlation between the melt factors and mean temperature for the 2000-2019 period is estimated ($r = -0.5$;

350 p-value = 0.08). Conversely, the correlation between the melt factors and mean precipitation for the 2000-2019
 351 period is high ($r = -0.8$; p-value = 0.002).

352 To test our results we evaluated the simulated mass balance evaluation for the 15 glaciers that can be found in
 353 Tables S4, S5 and Figures S3 and S4 of the Supplementary Materials. The *in situ* data show a mean negative
 354 mass balance (-832 ± 795 mm w.e. yr^{-1}) between 2000 and 2019 greater than our mean simulated mass balance
 355 (-647 ± 713 mm w.e. yr^{-1}) in the same glaciers. The evaluation results give a mean Pearson correlation of 0.67
 356 (except for Agua Negra, Ortigas 1, Guanaco and Amarillo glaciers, which shows either no correlation or a
 357 negative correlation) with an underestimation of the mean simulated mass balance of 185 mm w.e. yr^{-1} (bias);
 358 40% of the glaciers present a correlation equal to or greater than 0.7. In terms of the best results by glaciological
 359 region, in the Tropical Andes, the Conejeras glacier has a high correlation ($r = 0.9$) and bias (1104 mm w.e. yr^{-1}),
 360 whereas in the Dry Andes, the Piloto Este, Paula, Paloma Este and Del Rincón glaciers display a high correlation
 361 ($r \geq 0.8$) and a mean bias of 351 mm w.e. yr^{-1} . In the Wet Andes, the Mocho-Choshuencho and Martial Este
 362 glaciers show a moderate correlation ($r = 0.5$) and a lower overestimation of the simulated mass balance (-118
 363 mm w.e. yr^{-1}). Model limitations are observed on the Zongo glacier ($r = 0.3$ and bias = -224 mm w.e. yr^{-1}) in the
 364 Tropical Andes. In the Dry Andes 1, no correlation is observed in the three monitored glaciers (Guanaco,
 365 Amarillo and Ortigas 1); this is mainly because sublimation is very high on these glaciers, reaching 81% of the
 366 annual ablation (MacDonell et al., 2013). On the other hand, sublimation is lower southward in the Dry Andes 2
 367 with 7% of the annual ablation (Ayala et al., 2017). For the tropical zone, sublimation is close to 13% in Outer
 368 Tropics (Sicart et al., 2005) and 5% in Inner Tropics (Favier et al., 2004). However, sublimation is implicitly
 369 included in the model through the calibrated melt factor values, which are derived from measured mass balance
 370 data by Hugonnet et al. (2021). As a result, our estimates of snow/ice melt in the Dry Andes 1 zone tend to be
 371 overestimated.

372 The details of the glacier changes in the 786 Andean catchments, which are larger in the Wet Andes followed by
 373 the Tropical Andes and then the Dry Andes, are available in the Supplementary Materials.

374

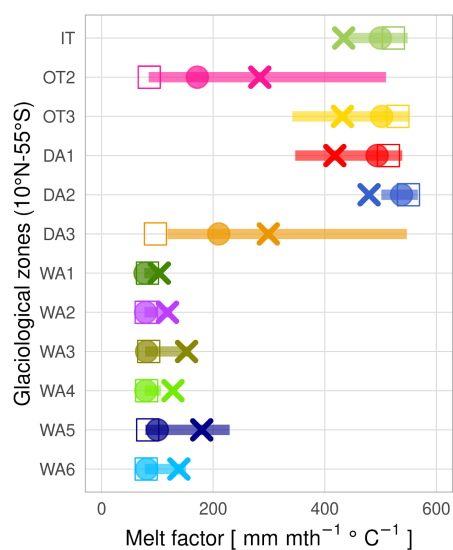


Figure 3. Statistics for the calibrated melt factors per glacier at the glaciological zone scale across the Andes. This figure shows the mean (x), median (circle), mode (square), and percentile 25 and 75 (lines) values for 13,179 glaciers.

375

376 3.3 Changes in glacier runoff across the Andes during the period 2000-2019

377 Due to glacier changes across the Andes, high glacier runoff variations are observed from glacier melt and
378 rainfall on glaciers (Figure 4). The mean annual glacier melt in all catchments for the period 2000-2019 was 696
379 m^3/s . At the regional scale, the Wet Andes shows the largest mean annual glacier melt in the Andes (583.5 m^3/s),
380 followed by the Dry Andes (59.9 m^3/s) and then the Tropical Andes (52.7 m^3/s). However, if we look at the mean
381 annual glacier melt changes between the periods 2000-2009 and 2010-2019, we see an increase of 12% (86.5
382 m^3/s) across the Andes, where 84% (n = 661) of catchments show an increase and 12% (n = 95) of them present
383 a decrease. As Table S6 shows, an increase in glacier melt is observed in catchments with a higher glacier
384 elevation, larger glacier size, lower mean temperature and higher mean precipitation compared with catchments
385 that show either a decrease in glacier melt or no changes at all. These latter catchments also show the largest
386 decrease in precipitation (-10 to -14%).

387 The mean annual glacier melt changes show the largest percentage increase in the Tropical Andes (40%, 21
388 m^3/s), followed by the Dry Andes (36%, 21.7 m^3/s), and the Wet Andes (8%, 4.8 m^3/s). In addition, significant
389 differences are observed for the different zones: for instance, the Inner Tropics in the Tropical Andes presents the
390 largest increase (73% with only 4.1 m^3/s), followed by Dry Andes 1 (62% with only 1.8 m^3/s) in the Dry Andes.
391 In the Wet Andes, the larger percentage of increase in the mean annual glacier melt changes is observed in Wet
392 Andes 5 (14% with 4.1 m^3/s), showing a lower percentage in comparison with the Inner Tropics and Dry Andes
393 1 zones, however, its absolute increase in glacier melt is equal to or greater than 4.1 m^3/s . These results per
394 glaciological zone are summarized in Table 2. Related to the previously described glacier changes (see Section
395 3.2) between the periods 2000-2009 and 2010-2019, at the glaciological zone scale, we logically find a high
396 negative correlation between the glacier melt and glacier volume changes in the Tropical Andes and Dry Andes
397 ($r = -0.9$) and the Wet Andes ($r = -1$).

398 In addition, the mean annual rainfall on glaciers across the Andes is 387 m^3/s for the period 2000-2019. The Wet
399 Andes has the largest amount of annual rainfall (372.7 m^3/s), followed by the Tropical Andes (10.5 m^3/s) and
400 Dry Andes (4.2 m^3/s) with the lowest contribution of rainfall.

401 In terms of the variations in the mean annual rainfall on glaciers between the periods 2000-2009 and 2010-2019,
402 we observe a reduction of -2% (-7.6 m^3/s) across the Andes, showing a reduction in 41% of the catchments (n =
403 322) whereas the largest proportion of the catchments (51%, n = 403) show an increase. Table S6 shows that the
404 catchments with the larger increase of rainfall on glaciers are concentrated in the same latitude range as the
405 catchments with an increase in glacier melt. These catchments have similar glacier elevations and glacier sizes.
406 The catchments that do not show variations in rainfall on glaciers are concentrated in the Dry Andes region,
407 where the rainfall contributes less to the glacier runoff volume.

408 At the glaciological region scale, the mean annual rainfall on glaciers decreases in the Wet Andes (-3%, 10.1
409 m^3/s), but increases in the Tropical Andes (23%, 2.4 m^3/s) and Dry Andes (3%, 0.1 m^3/s). In addition, large
410 differences are observed in the glaciological zones (Table 2): e.g. Dry Andes 1 in the Dry Andes has the largest

411 percentage increase (106% with only 0.2 m³/s), followed by Inner Tropics (74% with only 0.4 m³/s) in the
 412 Tropical Andes. In the Wet Andes, the larger increase (in percent) in the mean annual rain on the glaciers is
 413 observed in Wet Andes 5 (6.6% with 2.1 m³/s). Other zones such as Wet Andes 2 and Wet Andes 6 show large
 414 absolute reductions (-11.7 m³/s and -4.5 m³/s, respectively).
 415 The changes in glacier melt and rainfall on glaciers observed in the Tropical Andes, Dry Andes and Wet Andes
 416 are summarized in Table 2, and are available for the 786 Andean catchments in the Supplementary Materials.
 417

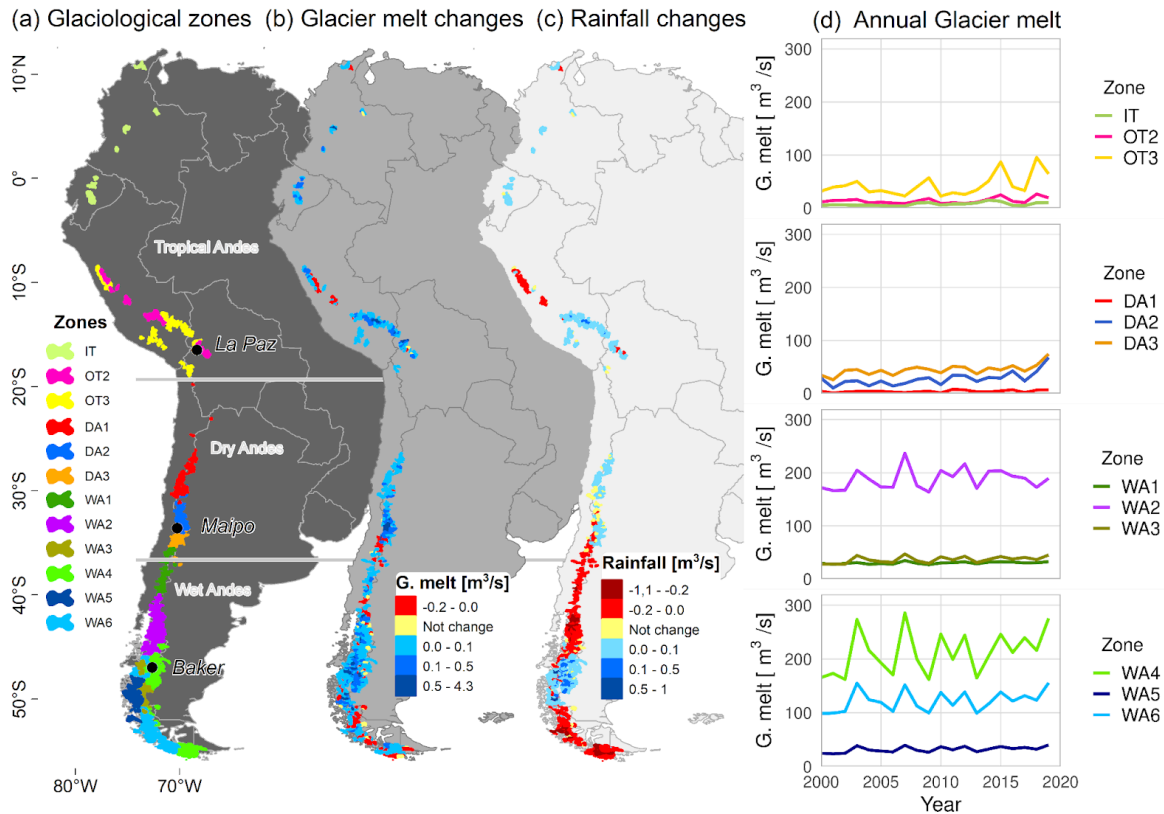


Figure 4. Recent glacier runoff components across the Andes. The total glacier melt and rainfall on glaciers represent the mean differences between the periods 2010-2019 and 2000-2009 per catchment (n = 786). (a) It shows the distribution of the glaciological zones (11°N-55°S), followed by (b) glacier melt and (c) rainfall on glaciers at the catchment scale. The (d) total annual glacier melt is presented in each glaciological zone. G. melt and Rainfall refer to changes in (b) Glacier melt and (c) Rainfall on glaciers, respectively, meanwhile, G. melt in the Y-axis in (d) refers to cumulative annual glacier melt by glaciological zone.

418

Table 2. Mean annual changes in glacier area and volume, glacier runoff and climate between periods 2000-2009 and 2010-2019 at the glaciological zones scale across the Andes (11°N-55°S)								
Region	Zone	Change in surface area [km ²] (%)	Change in volume [km ³] (%)	Change in glacier melt [m ³ /s] (%)	Change in rainfall on glaciers [m ³ /s] (%)	Simulated area [km ²] and percentage in total glacierized area (%)	cTCt change [°C]	cTCp change [mm yr ⁻¹] (%)
Tropical Andes	IT	-5.8 (-3)	-0.7 (-8)	4.1 (73)	0.4 (74)	191 (88)	0.6	81 (7.1)

	OT2	-19.3 (-4)	-1.2 (-8)	2.8 (23)	0.3 (10)	437 (77)	0.3	19 (2)
	OT3	-30.4 (-3)	-4 (-7)	14.1 (40)	1.6 (25)	1149 (81)	0.4	43 (5.2)
Dry Andes	DA1	-5.2 (-2)	-0.4 (-4)	1.8 (62)	0.2 (106)	218 (93)	0.3	50 (11.9)
	DA2	-7.4 (-1)	-2 (-4)	11.3 (59)	0.1 (14)	770 (76)	0.3	-269 (-32)
	DA3	-32.6 (-5)	-3 (-8)	8.5 (23)	-0.1 (-3)	613 (97)	0.3	-629 (-27.2)
Wet Andes	WA1	-7 (-3)	-1.1 (-8)	1.7 (6)	-1.6 (-13)	237 (93)	0.3	-937 (-18.3)
	WA2	-41.2 (-3)	-11.6 (-13)	10.7 (6)	-11.7 (-9)	1550 (91)	0.4	-454 (-8)
	WA3	-4.9 (-1)	-3 (-7)	4.4 (14)	1.1 (5)	469 (4)	0.5	-161 (-4.4)
	WA4	-72 (-2)	-21.4 (-9)	15.3 (8)	4.4 (5)	3746 (57)	0.4	-96 (-5.1)
	WA5	4.5 (1)	-0.3 (-1)	4.1 (14)	2.1 (7)	378 (15)	0.4	-407 (-6.5)
	WA6	-23.9 (-2)	-10.5 (-8)	7.7 (7)	-4.5 (-5)	1524 (32)	0.3	-382 (-10)

419 3.4 Hydro-glaciological behavior at the catchment scale during the period 2000-2019

420 In this Section, we focus on three Andean catchments: La Paz (16°S, Tropical Andes), Maipo (33°S, Dry Andes)
421 and Baker (47°S, Wet Andes) (see locations in Figure 2 or 4), where previous glaciological observations and
422 simulations of glacier evolution and water production have been carried out, and *in situ* records are also
423 available. Detailed results for each of the 786 catchments and glaciers included are available in the dataset
424 provided in the Supplementary Material.

425 3.4.1 Glaciological variations in the selected catchments: La Paz (16°S), Maipo (33°S) and Baker (47°S)

426 Figure 5 shows the annual specific mass balance in the three catchments (2000-2019). The mean over the study
427 period is negative, and there is a negative trend for the annual values toward 2019. For instance, for the Maipo
428 catchment, we estimate a mean annual mass balance of -0.29 ± 0.14 m w.e. yr^{-1} , a slightly more negative balance
429 in the Baker catchment (-0.47 ± 0.19 m w.e. yr^{-1}), whereas the glaciers in the La Paz catchment show a greater
430 loss of -0.56 ± 0.19 m w.e. yr^{-1} . In addition, when considering the annual mass balance values, it is possible to
431 note differences between the catchments. The La Paz catchment shows mostly negative annual mass balance
432 values over the whole period, while in the Baker and Maipo catchments the mass balances are predominantly
433 negative after 2004 and 2009, respectively. Considering the total area and volume changes per catchment in the
434 periods 2000-2009 and 2010-2019, an overall reduction is observed in each of the three catchments. For the La
435 Paz catchment, considering 86% (14 km²) of glacierized area in 2000 (mean glacierized elevation of 5,019 m
436 a.s.l.) and 20 glaciers, the glacierized surface area and volume decrease by -7% (-1 km²) and -11% (-0.1 km³),
437 respectively. For the Maipo catchment, with a larger percentage of simulated glacierized surface area in 2000

438 (99%, with mean elevation of 4,259 m a.s.l.) and a greater number of glaciers ($n = 225$), the area and volume
 439 decrease by -1% (-4.2 km^2) and -5% (-1 km^3), respectively. For the Baker catchment, which contains the largest
 440 glacierized surface area of the three catchments in 2000, we simulated 66% of this glacierized area (1514 km^2 ,
 441 with mean elevation of 1,612 m a.s.l.) and 1805 glaciers: this area shrank by approximately -2% (-36.7 km^2),
 442 losing close to -11% (-9.3 km^3) of its volume. These results are summarized in Table 3.
 443

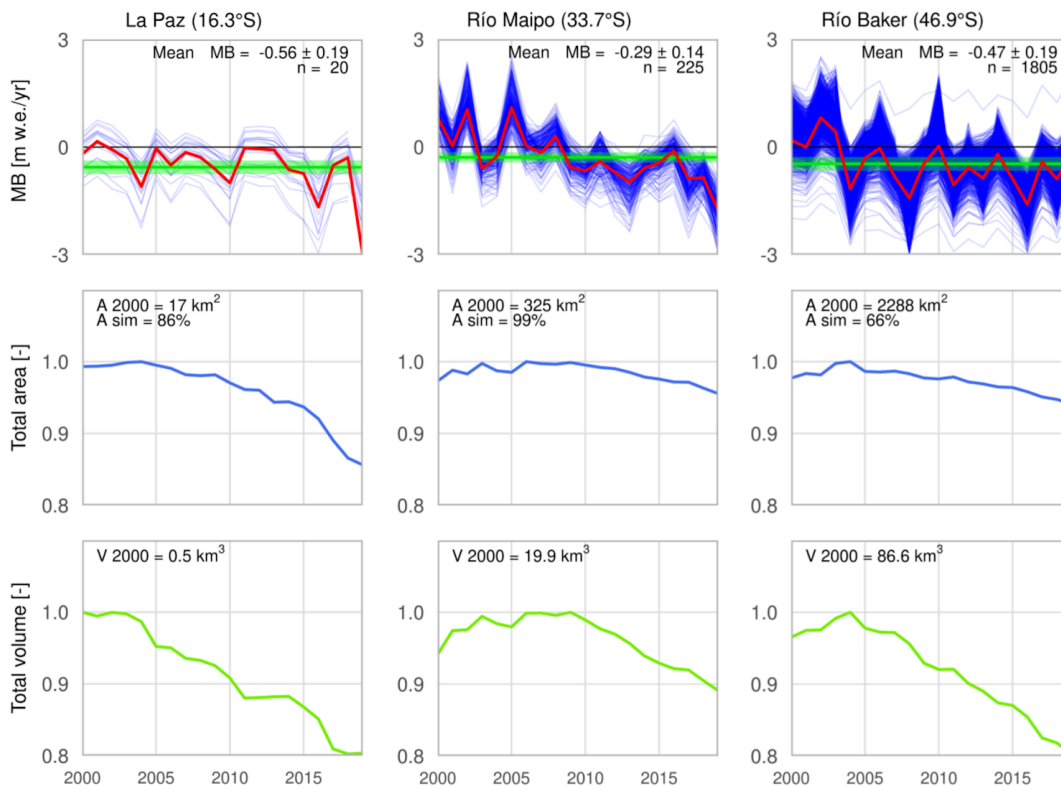


Figure 5. Recent annual specific mass balance, surface area, and volume variations in the La Paz, Maipo, and Baker catchments from 2000 to 2019. The first row shows the mass balance for each simulated glacier (blue line), as well as the weighted mean mass balance per catchment (red line). The mean geodetic mass balance and its error for the period 2000-2019 are also presented (green bar). The second row presents the total glacierized area per catchment (blue line). The total area from RGI v6.0 and the simulated area percentage are also presented. The last row exhibits the total volume per catchment (green line). The surface area and volume have both been normalized to make it easier to compare the evolution between the catchments.

444 3.4.2 Hydrological contribution of glaciers in the selected catchments: La Paz (16°S), Maipo (33°S) and 445 Baker (47°S)

446 The La Paz, Maipo, and Baker catchments display large climatic and glaciological differences over the period
 447 2000-2019. For instance, contrasting cumulative precipitation amounts can be found between the Baker and La
 448 Paz catchments ($2224 \pm 443 \text{ mm yr}^{-1}$ and $791 \pm 100 \text{ mm yr}^{-1}$, respectively), while the La Paz and Maipo
 449 catchments present the maximum difference in mean annual temperature ($1.4 \pm 0.5^\circ\text{C}$ and $-4.1 \pm 0.5^\circ\text{C}$,
 450 respectively) (Figure 6). At a seasonal scale, precipitation in the Maipo and Baker catchments is concentrated in
 451 autumn and winter (April-September), even if the latter catchment also has a significant amount of precipitation
 452 in summer. Conversely, precipitation in the La Paz catchment mainly occurs in spring and summer (October to

453 March). In addition, the La Paz and Baker catchments are characterized by the warmest temperatures ($>0^{\circ}\text{C}$) in
 454 spring and summer; the warmest temperatures for the Maipo catchment occur in summer. Variations in the
 455 climatic conditions are observed between 2000-2009 and 2010-2019. For instance, a decrease in cumulative
 456 precipitation is observed in the Maipo (-30%, -454 mm yr^{-1}) and Baker catchments (-2%, -52 mm yr^{-1}), but an
 457 increase can be seen in the La Paz catchment (4%, 30 mm yr^{-1}). The mean annual temperature increases in the
 458 three catchments ($+0.5^{\circ}\text{C}$ in La Paz and Baker, $+0.4^{\circ}\text{C}$ in Maipo).
 459 The glacier runoff simulation, which considers the glacier melt (ice and snow melt) and rainfall on glaciers
 460 (liquid precipitation), shows strong differences between the catchments (Figure 6). Over the period 2000-2019,
 461 the glaciers in the Baker catchment have the highest mean annual glacier melt ($94 \pm 19.6\text{ m}^3/\text{s}$), followed by
 462 those in the Maipo ($15.1 \pm 4.2\text{ m}^3/\text{s}$) and La Paz catchments ($0.5 \pm 0.2\text{ m}^3/\text{s}$). The rainfall on glaciers contributes
 463 30% to glacier runoff in the Baker catchment ($41 \pm 10.1\text{ m}^3/\text{s}$); a lower value is found in the La Paz catchment
 464 with 17% ($0.1\text{ m}^3/\text{s}$) followed by the Maipo catchment with 5% ($0.8 \pm 0.3\text{ m}^3/\text{s}$), which is the lowest contribution
 465 of rainfall on glaciers in these catchments. The simulations of glacier runoff changes between the periods
 466 2000-2009 and 2010-2019 for the three catchments show an increase in glacier melt and rainfall on glaciers. The
 467 largest relative increase in mean annual glacier melt is observed in the Maipo with 37% ($4.7\text{ m}^3/\text{s}$), followed by
 468 the La Paz with 21% ($0.09\text{ m}^3/\text{s}$) and the Baker catchments with 10% ($9\text{ m}^3/\text{s}$). Meanwhile, the largest relative
 469 increase in the mean annual rainfall on glaciers is observed in the La Paz catchment (15%, $0.01\text{ m}^3/\text{s}$), followed
 470 by the Baker catchment (11%, $4.3\text{ m}^3/\text{s}$) and lastly the Maipo catchment (2%, $0.02\text{ m}^3/\text{s}$). The results for the
 471 glacier melt and rainfall on glaciers are summarized in Table 3.
 472

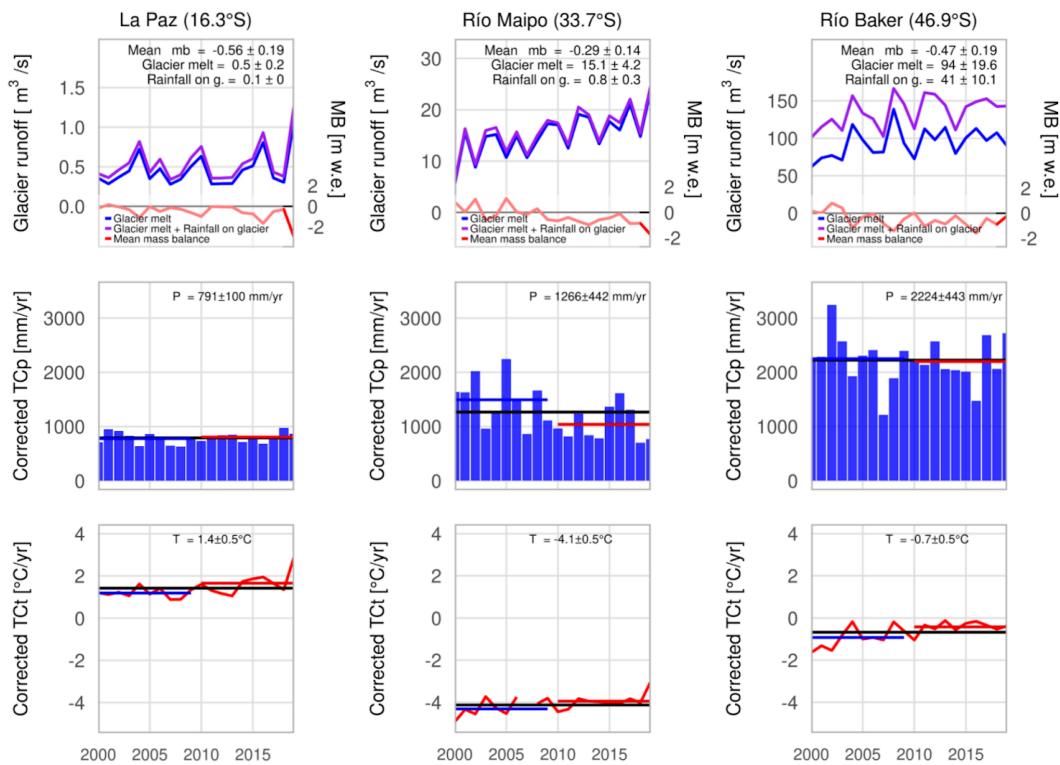


Figure 6. Hydro-glaciological responses and climate variations in the La Paz, Maipo and Baker catchments from 2000 to 2019. The first row presents the mean annual glacier runoff (purple line = ice melt+snow

melt+rainfall on glaciers), the mean annual glacier melt (blue line = ice melt+snow melt), and the annual specific mass balance (red line). The other rows show the mean total annual precipitation and mean annual temperature with the mean annual amount for the periods 2000-2019 (black line), 2000-2009 (blue line) and 2010-2019 (red line).

473

474 In Figure 7, at a mean monthly temporal scale for the period 2000-2019, the glacier melt simulation presents a
 475 short maximum during summer (January-February) in the Maipo and Baker catchments. In contrast, peaks in the
 476 La Paz catchment are extended during spring and summer (November-March) highlighting the so-called
 477 transition season (between September and November) where there is a low amount of rainfall on glaciers and
 478 glacier melt progressively increases. In the Baker catchment, melting begins earlier in September while in Maipo
 479 it begins later (November). The interannual variability of glacier melt over the periods 2000-2009 and
 480 2010-2019 shows a larger contribution from the glacier in the period 2010-2019 for the Maipo catchment.
 481 Furthermore, the simulated rainfall on glaciers is larger mainly during the summer season in all catchments, with
 482 more rainfall in the La Paz catchment (December to February) after the transition season.

483

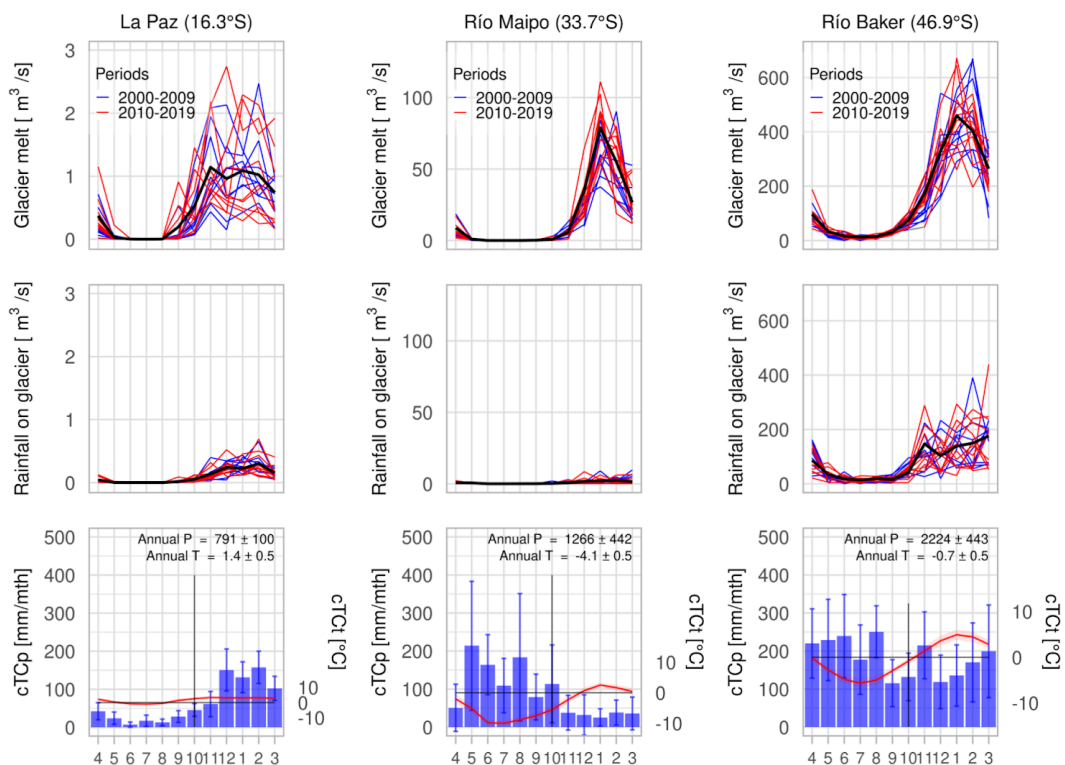


Figure 7. Monthly hydro-glaciological responses and climate variations in the La Paz, Maipo and Baker catchments from 2000 to 2019. The first and second rows present the mean monthly glacier melt and rainfall on glaciers (black line) and the mean amounts per year during the periods 2000-2009 (red lines) and 2010-2019 (blue lines). In the last row, the climographs show the mean monthly precipitation (blue bars) and temperature (red line) for the period 2000-2019.

484

485 For the mean annual discharge measurements in each catchment and the mean annual simulated glacier runoff
 486 (glacier melt and rainfall on glaciers) between 2000-2019 (Figure 8), we estimate that the largest glacier runoff
 487 contribution is in the Baker catchment (24%), followed by the La Paz (22%) and Maipo catchments (14%),
 488 where all catchments present a similar proportion of glacierized surface area (7.5% to 8.2%). If we consider the
 489 summer season only (January to March), the glacier runoff contribution is highest in the Baker catchment (43%),
 490 followed by the Maipo (36%) and La Paz catchments (18%), where the larger percentage of glacier melt is found
 491 in the Maipo catchment (34%) and the larger percentage of rainfall on glaciers is displayed in the Baker
 492 catchment (12%). Unlike the Maipo and Baker catchments, which present a maximum glacier runoff
 493 contribution in the summer season, the La Paz catchment shows the largest glacier runoff contribution (45%) in
 494 the transition season (September to November).

495

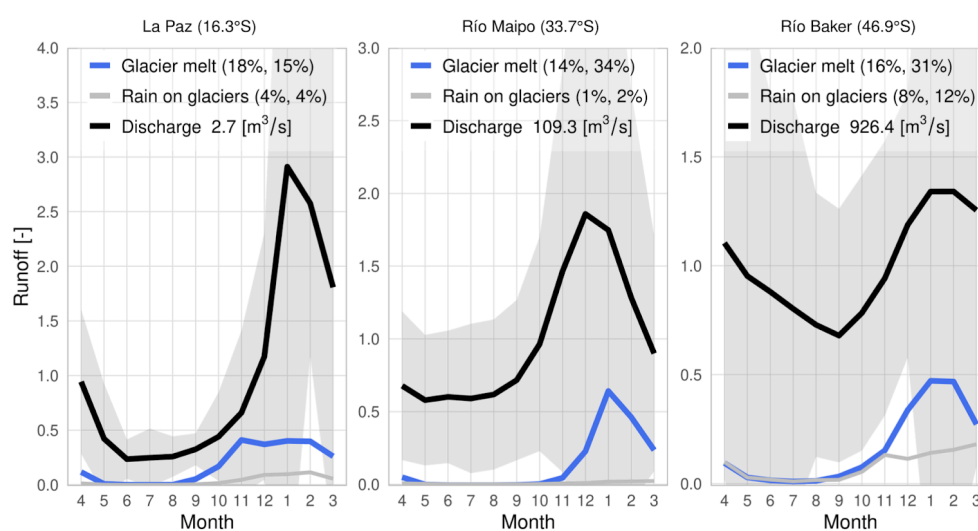


Figure 8. Monthly simulated glacier runoff (glacier melt + rainfall on glaciers) and discharge measurements in the La Paz, Maipo, and Baker catchments from 2000 to 2019. The results for the glacier melt (blue lines) and rainfall on glacier calculations (gray) are presented, as well as the discharge measurement (black line) and its standard deviation (gray area). The mean annual glacier runoff contribution (as a percentage) and the mean glacier runoff contribution (as a percentage) from January to March are shown in parentheses. The values are normalized by the mean river discharge.

496

Table 3. Hydro-glaciological changes and variations in climate between the periods 2000-2009 and 2010-2019 for the three selected catchments								
Region	Catchment	Change in surface area [km ²] (%)	Change in volume [km ³] (%)	Contribution of the annual glacier melt [m ³ /s] (%)	Contribution of the annual rainfall on glaciers [m ³ /s] (%)	Total simulated glacierized area [km ²] (%)	cTCt variation [°C]	cTCp variation [mm yr ⁻¹] (%)
TA	La Paz	-0.96 (-6.7)	-0.1 (-11.5)	0.09 (21.3)	0.01 (15.3)	14.4 (86)	0.5	30 (4)
DA	Maipo	-4.2 (-1.3)	-1 (-5)	4.7 (37)	0.02 (2.2)	353.9 (99)	0.4	-454 (-30)
WA	Baker	-36.7 (-2.4)	-9.3 (-10.7)	9 (10)	4.3 (11.2)	1514 (66)	0.5	-52 (-2)

497

498 4 Discussion

499 4.1 Comparison with previous studies across the Andes

500 Huss and Hock (2018) studied 12 Andean catchments across the Andes (1980-2000 and 2010-2030) and
501 estimated an increase in glacier runoff in the Tropical Andes (Santa and Titicaca catchments) and the Dry Andes
502 (Rapel and Colorado catchments). Our results are consistent with these estimates. We show an increase in glacier
503 melt by 40% and 36% in both regions, respectively, between the periods 2000-2009 and 2010-2019. However, in
504 the Wet Andes, Huss and Hock (2018) did not estimate any changes in glacier runoff on the western side of the
505 Andes (Biobio catchment), and instead found a decrease (Río Negro catchment) and an increase (Río Santa Cruz
506 catchment) in glacier runoff on the eastern side of the Andes. Our results for this region show an increase in
507 glacier melt by 8% and a decrease in rainfall on glaciers by -3%.

508 Based on local reports in the Tropical Andes, the catchment associated with the Los Crespos glacier (catchment
509 id = 6090223080) on the Antisana volcano shows a small decrease in the glacier area of -1% between the periods
510 2000-2009 and 2010-2019, which is in agreement with Basantes-Serrano et al. (2022). Their study estimated that
511 almost half of the glacier area (G1b, G2-3, G8, G9 and G17) had a positive mass balance during the period
512 1998-2009 with the largest glacier presenting a mass balance of 0.36 ± 0.57 m w.e. yr^{-1} , in agreement with our
513 mass balance estimation at the catchment scale of 0.2 ± 0.5 m w.e. yr^{-1} (2000-2009). However, in this region, the
514 corrected TerraClimate temperature cannot reproduce the magnitude of the monthly temperature variation (see
515 Figure S2). This limits the effectiveness of the parameter values used in the model to accurately simulate the
516 melting onset and the amount of solid/liquid precipitation. Furthermore, the mass balance simulation is
517 performed through the temperature-index model which does not take the sublimation process into account; and
518 in addition, it runs at a monthly time step thereby limiting the relevant processes that occur hourly. On the other
519 hand, the catchments that contain the Zongo glacier (catchment id = 6090629570) and the Charquini glacier
520 (catchment id = 6090641570) display results that are consistent with the observations (Rabatel et al., 2012;
521 Seehaus et al., 2020; Autin et al. 2022). In addition, our simulated mass balance evaluation on the Zongo glacier
522 shows a low bias (-0.2 m w.e. yr^{-1}) with regard to the observations. In the Dry Andes, the catchments associated
523 with the Pascua Lama area (catchment id = 6090836550 and catchment id = 6090840860), the Tapado glacier
524 (catchment id = 6090853340) and the glaciers of the Olivares catchment (catchment id = 6090889690) show
525 consistent results in terms glaciological variations in comparison with the observations (Rabatel et al., 2011;
526 Malmros et al., 2016; Farías-Barahona et al., 2020; Robson et al., 2022). In the Wet Andes, the catchments
527 associated with the Chilean side of the Monte Tronador (catchment id = 6090945100) and the Martial Este and
528 Alvear glaciers in Tierra del Fuego (catchment id = 6090037770) show results that are consistent with previous
529 reports (Rabassa 2010; Ruiz et al., 2017). Despite this, it is possible that our methodology could overestimate
530 precipitation in some catchments; for example, the cumulative precipitation associated with the Nevados de
531 Chillán catchment (catchment id = 6090916140) was estimated at 4023 mm yr^{-1} .

532 At the glaciological region scale, previous studies have reported a large decrease in the percentage of glacier area
533 in the Tropical Andes by -29% (2000-2016) (Seehaus et al., 2019; 2020), followed by the Dry Andes between
534 -29 and -30% (Rabatel et al., 2011; Malmros et al., 2016) although for a longer time-period. In the Wet Andes,
535 Meier et al. (2018) reported a -9% decrease in the glacier area (1986–2016). Our simulations are consistent with
536 these observed glacier area reductions. In addition, Caro et al. (2021) estimated a similar trend across the Andes
537 between 1980-2019 (Tropical Andes = -41%, Dry Andes = -39%, Wet Andes = -24%). On the other hand, we

538 found high correlations between the mean annual climatic variables and annual mass balance. In the Dry Andes,
539 this correlation was high with precipitation ($r = 0.8 \pm 0.1$, p -value < 0.05) and in the Wet Andes, temperature was
540 correlated with mass balance ($r = -0.7 \pm 0.1$, p -value < 0.05) as previously observed by Caro et al. (2021). These
541 correlations between precipitation or temperature with the annual mass balances for each catchment across the
542 Andes can be reviewed in Table S7 and Figure S5 of the Supplementary Materials.

543 4.2. Comparison of our results with previous studies in the three selected catchments

544 In the La Paz catchment, Soruco et al. (2015) evaluated the mass balance of 70 glaciers (1997-2006) and their
545 contribution to the hydrological regime. In the present study, we simulated a less negative mass balance ($-0.56 \pm$
546 0.19 m w.e. yr^{-1} vs. -1 m w.e. yr^{-1}) considering a larger glacierized area due to the use of RGI v6.0 (with 14.1 km^2
547 in comparison to 8.3 km^2). Our estimation of the mean annual glacier runoff (22%) is larger than the previous
548 estimation close to 15% (Soruco et al., 2015). This may be due to the fact that we have considered a warmer
549 2010-2019 period than the one observed in Soruco et al. (2015). Unlike the previous report, we estimated a
550 larger glacier runoff contribution during the wet season (26%, October to March) and increasing in the transition
551 season (45%, September to November). This increase in glacier runoff contribution given by the model agrees
552 with the larger glacier mass loss observed by Sicart et al. (2007) and Autin et al. (2022) during this season. In the
553 Maipo catchment, we identified a slightly smaller glacierized area (325 km^2 for the year 2000, -14%) compared
554 with Ayala et al. (2020) because they considered rock glaciers from the Chilean glacier inventory. In addition, we
555 observed a more negative mass balance after 2008, coinciding with the mega-drought period characterized by a
556 decrease in precipitation and an increase in temperature (Garreaud et al., 2017). The hydrological response to
557 this negative mass balance trend is an increase in glacier runoff since 2000 that is concentrated between
558 December and March. The modeled mean annual glacier runoff contribution estimation is close to 15%, reaching
559 36% in summer (January-March), is close to Ayala et al. (2020) estimation (16% at the annual scale for the
560 period 1955-2016). However, this comparison between our results and previous studies in the Maipo and La Paz
561 catchments is limited due to the utilization of different inputs, spatial resolutions, time steps, and workflow in the
562 simulated processes where some processes as mass balance of all glaciers was not done. Lastly, in the Baker
563 catchment, Dussaillant et al. (2012) stated that catchments associated with the Northern Patagonian Icefield
564 (NPI) are strongly conditioned by glacier melting. In this respect, Huss and Hock (2018) did not identify glacier
565 runoff changes between the periods 1980-2000 and 2010-2030, they only considered 183 km^2 of the glacierized
566 area (-12% until 2020), whereas we estimated a 10% and 11% increase in glacier melt and rainfall on glaciers,
567 respectively, taking a larger glacierized area (1514 km^2 ; -2% until 2020) into account. The relevance of the
568 rainfall on glaciers with regards to the glacier runoff estimated here is close to 30% (including glaciers from east
569 of NPI to the east) which is confirmed by Krogh et al. (2014), who estimated that over 68% of the total
570 precipitation at the catchment scale in east NPI (León and Delta catchments) corresponds to rainfall.

571 4.3 Simulation limitations

572 Limitations in the simulations result from different sources: (1) the quality/accuracy of the input data; (2) the
573 calibration of the precipitation and melt factors; and (3) the model itself, including its structure and the processes
574 that are not represented. Regarding the evaluation of the corrected TerraClimate temperature using
575 meteorological observations in the Tropical Andes, the corrected TerraClimate data do not reproduce either the

576 low monthly temperature or the higher temperature in specific months which have a mean bias of 2.1°C (e.g.
577 Llan_Up-2 9°S, Zongo at glacier station 16°S). These differences found in the corrected TerraClimate data limit
578 the capacity of the ice/snow melting module to accurately simulate the months in which melting can occur. To
579 account for this, the values of the thresholds used for the melting onset and for the solid/liquid precipitation
580 phase have been adjusted and are described in the limitations (2). On the contrary, in the Dry Andes and Wet
581 Andes, the corrected TerraClimate temperatures are closer to the *in situ* observations (mean bias = 0.2°C) and
582 present a reliable monthly distribution. This results in model parameter values that are in better agreement with
583 the values used in other studies. Other limitations come from RGI v6.0 because some glaciers are considered as
584 only one larger glacier. For example, in the Dry Andes (catchment id = 6090889690) two large glaciers, the
585 Olivares Gamma and the Juncal Sur, form one (even larger) glacier. These glaciers could underestimate the
586 simulated change in glacier area, limiting the performance of the volume module which depends on the glacier
587 geometry and bedrock shape.

588 Furthermore, we applied different precipitation factor values in the Tropical Andes (1), Dry Andes (1.9 to 4) and
589 Wet Andes (2.3 to 4), in order to increase the annual mass balance. These values are in agreement with former
590 studies, for example, similar values were used in the Dry Andes (Masiokas et al., 2016; Burger et al., 2019;
591 Farías-Barahona et al., 2020). Values that are too high could lead to an overestimation of precipitation on some
592 glaciers. However, to confirm that the precipitation factor produces realistic precipitation values, we adjusted the
593 standard deviation of the simulated mass balance to the observed mass balance, a method similar to that
594 proposed in Marzeion et al. (2012) and Maussion et al. (2019). On the other hand, the uncertainty of the
595 calibrated melt factors come from the climate and geodetic mass balance datasets used to run and calibrate the
596 model. Indeed, the melting temperature threshold establishes the onset of melting and influences the number of
597 months in which it occurs. On the other hand, the geodetic mass balance defines the accumulated gain or loss per
598 glacier over the calibration period, which in this case spans 20 years. Based on our evaluation of the corrected
599 TerraClimate temperature and simulated mass balance, we correctly reproduce the seasonal melt distribution,
600 associated with a mean underestimated overall annual mass balance of 185 mm w.e. yr⁻¹ which however is
601 correlated with the *in situ* data ($r = 0.7$). According to Rounce et al. (2020), similar results of glacier surface
602 mass balance could be due to different combinations of model parameters. For instance, a wetter (or dryer) and
603 warmer (or colder) parameter set—where high (or low) precipitation factors are compensated by high (or low)
604 temperature biases—can lead to similar recent glacier mass changes and projections. Conversely, the
605 implications for glacier runoff are likely to be significant for both recent and future simulations. In a wetter (or
606 dryer) and warmer (or colder) scenario, there would be increased (or decreased) precipitation and melt, resulting
607 in larger (or smaller) glacier runoff contribution. To address this, we obtained realistic values for precipitation
608 and temperature based on *in situ* spatially distributed measurements and on our field experiences on monitored
609 Andean glaciers. Furthermore, our evaluation of simulations in the three selected catchments enabled us to
610 estimate glacier runoff amounts in the same order of magnitude as previous reports. However, caution must be
611 exercised when using the calibrated melt factors estimated in the Tropical Andes. This is because the temperature
612 in this region was overestimated by an average of 2.4°C, impacting the calibration of the melt factor values.
613 These values should be lower than those estimated here (see Figure 3).

614 With regards to the structural limitations of the model, it would be relevant to distinguish between ice and snow
615 melt when simulating the glacier melt with two melt factors. In addition, the sublimation on the glacier surface is

616 very relevant in some glaciers located in the Tropical Andes and Dry Andes 1 (Rabatel et al., 2011; MacDonnell
617 et al., 2013). However, the OGGM model does not incorporate these processes in glacier runoff and mass
618 balance simulations.

619 5 Conclusion

620 In this study, we present a detailed quantification of the glacio-hydrological evolution across the Andes
621 (11°N-55°S) over the period 2000-2019 using OGGM. Our simulations rely on a glacier-by-glacier calibration of
622 the changes in glacier volume. Simulations cover 11,282 km² of the glacierized surface area across the Andes,
623 taking out account that calving glaciers (mostly in the Patagonian icefields and Cordillera Darwin) were not
624 considering because calving is not accounted for in the version of glaciological model used here. The simulations
625 were performed for the first time employing the same methodological approach, a corrected climate forcing and
626 parameters calibration at the glaciological zone scale throughout the Andes. Evaluation of our simulation outputs
627 spanned glacier-specific and catchment-scale, integrating *in situ* observations -which is uncommon in regional
628 studies. From our results, we can conclude the following:

- 629 • In relation to glacier runoff composed by glacier melt and rainfall on glacier at the catchment scale; the
630 largest percentage of studied Andean catchments encompassing 84% of total (661 catchments)
631 presented an increase in 12% of the mean annual glacier melt (ice and snowmelt) between the periods
632 2000-2009 and 2010-2019. These catchments present glaciers with higher elevation, larger size and also
633 a lower mean annual temperature and higher mean annual precipitation compared with glaciers located
634 in catchments that showed a decrease in glacier melt in the same period which comprise just 12% of
635 studied catchments. Additionally, the mean annual rainfall on glacier between the periods 2000-2009
636 and 2010-2019 exhibited a reduction of -2%.
- 637 • Special attention must be directed towards the Tropical and Dry Andes regions, as they exhibited the
638 most significant percentage increase in glacier runoff between the periods 2000-2009 and 2010-2019,
639 reaching up to 40% due to glacier melt, and 3% due to increased rainfall on glacier over the past
640 decade. Specifically, the Dry Andes 1 showcased a remarkable 62% increase, while the Inner Tropic
641 zone exhibited a 73% rise in glacier runoff in the same periods. Notably, these particular glaciological
642 zones displayed the smallest absolute quantities of glacier runoff across the entire Andes region. The
643 Dry Andes 1 zone emerges as the most vulnerable glaciological zone to glacier runoff water scarcity in
644 the Andes.
- 645 • Three catchments (La Paz, Maipo and Baker) located in contrasted climatic and morphometric zones
646 (glaciological zones) are used to evaluate the simulations. Our results show consistency with previous
647 studies and *in situ* observations. The larger glacier runoff contributions to the catchment water flows
648 during the period 2000-2019 are quantified for the Baker (43%) and Maipo (36%) catchments during
649 the summer season (January-March). On the other hand, the larger glacier runoff contribution to the La
650 Paz catchment (45%) was estimated during the transition season (September to November).
- 651 • The correction of temperature and precipitation data, coupled with parameter calibration conducted at
652 the glaciological zone scale, enabled obtaining annual estimates of glacier mass balance and runoff
653 closer to what has been measured in glaciers and some Andean catchments. Highlighting the estimation
654 of annual temperature lapse rates and variability in glacier mass balance through measurements to

655 correct climate data across distinct glaciological zones. This improvement not only ensures better
656 alignment with local observations but also establishes a more robust tool for forecasting future glacier
657 runoff patterns in the Andes. This method stands apart from global models by specifically addressing
658 the local climate and parameter values inherent to the Andean region.

659 Lastly, our results help to improve knowledge about the hydrological responses of glacierized catchments across
660 the Andes through the correction of inputs, calibration by glaciers and validation of our simulations considering
661 different glaciological zones. The implementation of this model during the historical period is a prerequisite for
662 simulating the future evolution of the Andean glaciers.

663 **Code and data availability**

664 Data per glacier in this study is available at <https://doi.org/10.5281/zenodo.7890462>

665 **Supplement link**

666 Supplementary information is available at <https://doi.org/10.5194/egusphere-2023-888-supplement>

667 **Author contributions**

668 AC, TC and AR were involved in the study design. AC wrote the model implementation and produced the
669 figures, tables and first draft of the manuscript. NC contributed to the model implementation. AC and NG carried
670 out the data curation and TerraClimate temperature evaluation. AC performed the first level of analysis, which
671 was improved by input from TC, AR, NC, FS. All authors contributed to the review and editing of the
672 manuscript.

673 **Acknowledgments**

674 We acknowledge LabEx OSUG@2020 (Investissement d'Avenir, ANR10 LABX56). The first author would like
675 to thank Dr. Shelley MacDonell (University of Canterbury - CEAZA), Ashley Apey (Geostudios), Dr. Marius
676 Schaefer (U. Austral de Chile), and Dr. Claudio Bravo and Sebastián Cisternas (CECs, Centro de Estudios
677 Científicos de Valdivia) for the data provided. In addition, the first author thanks the OGGM support team,
678 especially Patrick Schmitt, Dr. Lilian Schuster, Larissa van der Laan, Anouk Vlug, Dr. Rodrigo Aguayo and Dr.
679 Fabien Maussion. Lastly, the first author greatly appreciates discussing the results for specific glaciers or
680 catchments with Dr. Ezequiel Toum (IANIGLA, Argentina), Dr. Álvaro Ayala (CEAZA, Chile), Dr. Lucas Ruiz
681 (IANIGLA, Argentina), Dr. Gabriella Collao (IGE, Univ. Grenoble Alpes, France), Dr. Diego Cusicanqui
682 (IGE-ISTerre, Univ. Grenoble Alpes, France), and Dr. David Farías-Barahona (FAU, U. de Concepción, Chile).
683 All authors are grateful for the comments provided by the two anonymous reviewers and by the editor, which
684 helped considerably improve the scientific quality of this article.

685 **Financial support**

686 This study was conducted as part of the International Joint Laboratory GREAT-ICE, a joint initiative of the IRD,
687 universities/institutions in Bolivia, Peru, Ecuador and Colombia, and the IRN-ANDES-C2H. This research was
688 funded by the National Agency for Research and Development (ANID)/Scholarship Program/DOCTORADO
689 BECAS CHILE/2019-72200174.

690 References

691 Abatzoglou, J. T., Dobrowski, S. Z., Parks, S. A., and Hegewisch, K. C. TerraClimate, a High-Resolution Global
692 Dataset of Monthly Climate and Climatic Water Balance from 1958-2015. *Sci. Data* 5, 1–12.
693 <https://doi.org/10.1038/sdata.2017.191>, 2018.

694

695 Alvarez-Garreton, C., Mendoza, P. A., Boisier, J. P., Addor, N., Galleguillos, M., Zambrano-Bigiarini, M., Lara,
696 A., Puelma, C., Cortes, G., Garreaud, R., McPhee, J., and Ayala, A.: The CAMELS-CL dataset: catchment
697 attributes and meteorology for large sample studies – Chile dataset, *Hydrol. Earth Syst. Sci.*, 22, 5817–5846,
698 <https://doi.org/10.5194/hess-22-5817-2018>, 2018.

699

700 Autin, P., Sicart, J. E., Rabatel, A., Soruco, A., and Hock, R. Climate Controls on the Interseasonal and
701 Interannual Variability of the Surface Mass and Energy Balances of a Tropical Glacier (Zongo Glacier, Bolivia,
702 16° S): New Insights From the Multi-Year Application of a Distributed Energy Balance Model. *Journal of*
703 *Geophysical Research: Atmospheres*, 127(7), <https://doi.org/10.1029/2021JD035410>, 2022.

704

705 Ayala, Á., Pellicciotti, F., MacDonell, S., McPhee, J., Burlando, P. Patterns of glacier ablation across
706 North-Central Chile: Identifying the limits of empirical melt models under sublimation-favorable conditions.
707 *Water Resources Research*, 53(7), 5601– 5625. <https://doi.org/10.1002/2016WR020126>, 2017.

708

709 Ayala, Á., Fariás-Barahona, D., Huss, M., Pellicciotti, F., McPhee, J., and Farinotti, D. Glacier Runoff Variations
710 since 1955 in the Maipo River Basin, Semiarid Andes of central Chile. *Cryosphere Discuss.* 14, 1–39.
711 <https://doi.org/10.5194/tc-2019-233>, 2020.

712

713 Baraer, M., Mark, B. G., Mckenzie, J. M., Condom, T., Bury, J., Huh, K.-I., et al. Glacier Recession and Water
714 Resources in Peru's Cordillera Blanca. *J. Glaciol.* 58 (207), 134–150. <https://doi.org/10.3189/2012JoG11J186>,
715 2012.

716

717 Basantes-Serrano, R., Rabatel, A., Francou, B., Vincent, C., Soruco, A., Condom, T., and Ruíz, J. C.: New
718 insights into the decadal variability in glacier volume of a tropical ice cap, Antisana (0°29' S, 78°09' W),
719 explained by the morpho-topographic and climatic context, *The Cryosphere*, 16, 4659–4677,
720 <https://doi.org/10.5194/tc-16-4659-2022>, 2022.

721

722 Bravo, C., Loriaux, T., Rivera, A., & Brock, B. W. Assessing glacier melt contribution to streamflow at
723 Universidad Glacier, central Andes of Chile. *Hydrology and Earth System Sciences*, 21(7), 3249-3266.
724 <https://doi.org/10.5194/hess-21-3249-2017>, 2017.

725

726 Braun, L. N. and Renner, C. B. Application of a conceptual runoff model in different physiographic regions of
727 Switzerland. *Hydrol. Sci. J.* 37(3), 217-231. 1992.

728

729 Burger, F., Ayala, A., Farias, D., Shaw, T. E., MacDonell, S., Brock, B., et al. Interannual Variability in Glacier
730 Contribution to Runoff from a High-elevation Andean Catchment: Understanding the Role of Debris Cover in
731 Glacier Hydrology. *Hydrological Process.* 33 (2), 214–229. <https://doi.org/10.1002/hyp.13354>, 2019.

732

733 Caro, A., Condom, T. and Rabatel, A. Climatic and Morphometric Explanatory Variables of Glacier Changes in
734 the Andes (8–55°S): New Insights From Machine Learning Approaches. *Front. Earth Sci.* 9:713011.
735 <https://doi.org/10.3389/feart.2021.713011>, 2021.

736

737 Caro, A. Estudios glaciológicos en los nevados de Chillán. Santiago: University of Chile. [thesis].
738 <https://repositorio.uchile.cl/handle/2250/116536>, 2014.

739

740 Cauvy-Fraunié, S., and Dangles, O. A Global Synthesis of Biodiversity Responses to Glacier Retreat. *Nat. Ecol.*
741 *Evol.* 3 (12), 1675–1685. <https://doi.org/10.1038/s41559-019-1042-8>, 2019.

742

743 CEAZA, datos meteorológicos de Chile [data set], <http://www.ceazamet.cl/>, 2022.

744

745 CECs. Meteorological data measured by Centro de Estudios Científicos, 2018.

746

747 Condom, T., Escobar, M., Purkey, D., Pouget J.C., Suarez, W., Ramos, C., Apaestegui, J., Zapata, M., Gomez, J.
748 and Vergara, W. Modelling the hydrologic role of glaciers within a Water Evaluation and Planning System
749 (WEAP): a case study in the Rio Santa watershed (Peru). *Hydrol. Earth Syst. Sci. Discuss.*, 8, 869–916.
750 <https://doi.org/10.5194/hessd-8-869-2011>, 2011.

751

752 Crippen, R., Buckley, S., Agram, P., Belz, E., Gurrola, E., Hensley, S., Kobrick, M., Lavalley, M., Martin, J.,
753 Neumann, M., Nguyen, Q., Rosen, P., Shimada, J., Simard, M., Tung, W. NASADEM Global Elevation Model:
754 Methods and Progress. *The International Archives of the Photogrammetry, Remote Sensing and Spatial*
755 *Information Sciences XLI-B4*, 125–128. (20), 2016.

756

757 Devenish, C., and Gianella, C. Sustainable Mountain Development in the Andes. 20 Years of Sustainable
758 Mountain Development in the Andes - from Rio 1992 to 2012 and beyond. Lima, Peru: CONDESAN, 2012.

759

760 DGA, datos de estudios hidroglaciológicos de Chile [data set], <https://snia.mop.gob.cl/BNAConsultas/reportes>,
761 2022.

762

763 Dussaillant A., Buytaert W., Meier C. and Espinoza F. Hydrological regime of remote catchments with extreme
764 gradients under accelerated change: the Baker basin in Patagonia. *Hydrological Sciences Journal*, Volume 57,
765 <https://doi.org/10.1080/02626667.2012.726993>, 2012.

766

767 Dussaillant, I., Berthier, E., Brun, F., Masiokas, M., Hugonnet, R., Favier, V., et al. Two Decades of Glacier Mass
768 Loss along the Andes. *Nat. Geosci.* 12 (10), 802–808. <https://doi.org/10.1038/s41561-019-0432-5>, 2019.

769

770 Farías-Barahona, D., Wilson, R., Bravo, C., Vivero, S., Caro, A., Shaw, T. E., et al. A Near 90-year Record of the
771 Evolution of El Morado Glacier and its Proglacial lake, Central Chilean Andes. *J. Glaciol.* 66, 846–860.
772 <https://doi.org/10.1017/jog.2020.52>, 2020.

773

774 Farinotti, D., Huss, M., Fürst, J. J., Landmann, J., Machguth, H., Maussion, F., et al. A consensus estimate for
775 the ice thickness distribution of all glaciers on Earth. *Nat. Geosci.* 12, 168–173.
776 <https://doi.org/10.1038/s41561-019-0300-3>, 2019.

777

778 Farinotti, D., Brinkerhoff, D. J., Clarke, G. K., Fürst, J. J., Frey, H., Gantayat, P. & Andreassen, L. M. How
779 accurate are estimates of glacier ice thickness? Results from ITMIX, the Ice Thickness Models Intercomparison
780 eXperiment. *The Cryosphere*, 11(2), 949-970, <https://doi.org/10.5194/tc-11-949-2017>, 2017.

781

782 Favier, V., Wagnon, P., Chazarin, J.-P., Maisincho, L., and Coudrain, A. One-year measurements of surface heat
783 budget on the ablation zone of Antizana glacier 15, Ecuadorian Andes, *J. Geophys. Res.*, 109, D18105,
784 <https://doi.org/10.1029/2003JD004359>, 2004.

785

786 Fukami, H. and Naruse, R. Ablation of ice and heat balance on Soler glacier, Patagonia. *Bull. Glacier Res.* 4,
787 37–42, 1987.

788

789 Gao L., Bernhardt M. and Schulz K. Elevation correction of ERA-Interim temperature data in complex terrain.
790 *Hydrol. Earth. Syst. Sci.* 16(12): 4661–4673, <https://doi.org/10.5194/hess-16-4661-2012>, 2012.

791

792 Garreaud, R. D., Alvarez-Garreton, C., Barichivich, J., Boisier, J. P., Christie, D., Galleguillos, M., LeQuesne,
793 C., McPhee, J., and Zambrano-Bigiarini, M.: The 2010–2015 megadrought in central Chile: impacts on regional
794 hydroclimate and vegetation, *Hydrol. Earth Syst. Sci.*, 21, 6307–6327,
795 <https://doi.org/10.5194/hess-21-6307-2017>, 2017.

796

797 Gascoïn, S., Kinnard, C., Ponce, R., Lhermitte, S., MacDonell, S., and Rabatel, A.: Glacier contribution to
798 streamflow in two headwaters of the Huasco River, Dry Andes of Chile, *The Cryosphere*, 5, 1099–1113,
799 <https://doi.org/10.5194/tc-5-1099-2011>, 2011.

800

801 GLACIOCLIM, Données météorologiques [data set], <https://glacioclim.osug.fr/Donnees-des-Andes>, 2022.

802

803 Guido, Z., McIntosh, J. C., Papuga, S. A., and Meixner, T. Seasonal Glacial Meltwater Contributions to Surface
804 Water in the Bolivian Andes: A Case Study Using Environmental Tracers. *J. Hydrol. Reg. Stud.* 8, 260–273.
805 <https://doi.org/10.1016/j.ejrh.2016.10.002>, 2016.

806

807 Hernández, J., Mazzorana, B., Loriaux, T., and Iribarren, P. Reconstrucción de caudales en la Cuenca Alta del
808 Río Huasco, utilizando el modelo Cold Regional Hydrological Model (CRHM), AAGG2021, 2021.

809

810 Hock, R. Temperature index melt modelling in mountain areas. *Journal of Hydrology*, 282(1-4), 104-115.
811 [https://doi.org/10.1016/S0022-1694\(03\)00257-9](https://doi.org/10.1016/S0022-1694(03)00257-9), 2003.

812

813 Hugonnet, R., McNabb, R., Berthier, E. et al. Accelerated global glacier mass loss in the early twenty-first
814 century. *Nature* 592, 726–731. <https://doi.org/10.1038/s41586-021-03436-z>, 2021.

815

816 Huss, M. and Hock, R. A new model for global glacier change and sea-level rise, *Front. Earth Sci.*, 3, 54,
817 <https://doi.org/10.3389/feart.2015.00054>, 2015.

818

819 Huss, M. and Hock, R. Global-scale hydrological response to future glacier mass loss, *Nature Climate Change*,
820 8, 135–140, <https://doi.org/10.1038/s41558-017-0049-x>, 2018.

821

822 IANIGLA, datos meteorológicos [data set], <https://observatorioandino.com/estaciones/>, 2022.

823

824 Kienholz, C., Rich, J. L., Arendt, A. A., and Hock, R.: A new method for deriving glacier centerlines applied to
825 glaciers in Alaska and northwest Canada, *The Cryosphere*, 8, 503–519, <https://doi.org/10.5194/tc-8-503-2014>,
826 2014.

827

828 Koizumi, K. and Naruse R. Measurements of meteorological conditions and ablation at Tyndall Glacier,
829 Southern Patagonia, in December 1990. *Bulletin of Glacier Research*, 10, 79-82, 1992.

830

831 Krögh, S.A., Pomeroy, J.W., McPhee, J. Physically based hydrological modelling using reanalysis data in
832 Patagonia. *J. Hydrometeorol.* <http://dx.doi.org/10.1175/JHM-D-13-0178.1>, 2014.

833

834 Lehner B, Verdin K, Jarvis A. Hydrological data and maps based on Shuttle elevation derivatives at multiple
835 scales (HydroSHEDS)-Technical Documentation, World Wildlife Fund US, Washington, DC, Available at
836 <http://hydrosheds.cr.usgs.gov>, 2016.

837

838 MacDonell, S., Kinnard, C., Mölg, T., Nicholson, L., and Abermann, J. Meteorological drivers of ablation
839 processes on a cold glacier in the semi-arid Andes of Chile, *The Cryosphere*, 7, 1513–1526,
840 <https://doi.org/10.5194/tc-7-1513-2013>, 2013.

841

842 Malmros, J. K., Mernild, S. H., Wilson, R., Yde, J. C., and Fensholt, R. Glacier Area Changes in the central
843 Chilean and Argentinean Andes 1955-2013/14. *J. Glaciol.* 62, 391–401. <https://doi.org/10.1017/jog.2016.43>,
844 2016.

845

846 Marangunic C., Ugalde F., Apey A., Armendáriz I., Bustamante M. and Peralta C. Ecosistemas de montaña de la
847 cuenca alta del río Mapocho, Glaciares en la cuenca alta del río Mapocho: variaciones y características
848 principales. AngloAmerican - CAPES UC, 2021.

849

850 Mark, B. and Seltzer, G. Tropical glacier meltwater contribution to stream discharge: A case study in the
851 Cordillera Blanca, Peru. *J. Glaciol.* 49(165), 271-281. <https://doi.org/10.3189/172756503781830746>, 2003.

852

853 Marzeion, B., Jarosch, A. H., and Hofer, M.: Past and future sea-level change from the surface mass balance of
854 glaciers, *The Cryosphere*, 6, 1295–1322, <https://doi.org/10.5194/tc-6-1295-2012>, 2012.

855

856 Masiokas, M. H., Christie, D. A., Le Quesne, C., Pitte, P., Ruiz, L., Villalba, R., et al. Reconstructing the Annual
857 Mass Balance of the Echaurren Norte Glacier (Central Andes, 33.5° S) Using Local and Regional Hydroclimatic
858 Data. *The Cryosphere* 10 (2), 927–940. <https://doi.org/10.5194/tc-10-927-2016>, 2016.

859

860 Masiokas, M. H., Rabatel, A., Rivera, A., Ruiz, L., Pitte, P., Ceballos, J. L., et al. A Review of the Current State
861 and Recent Changes of the Andean Cryosphere. *Front. Earth Sci.* 8 (6), 1–27.
862 <https://doi.org/10.3389/feart.2020.00099>, 2020.

863

864 Mateo, E. I., Mark, B. G., Hellström, R. Å., Baraer, M., McKenzie, J. M., Condom, T., Rapre, A. C., Gonzales,
865 G., Gómez, J. Q., and Encarnación, R. C. C.: High-temporal-resolution hydrometeorological data collected in the
866 tropical Cordillera Blanca, Peru (2004–2020), *Earth Syst. Sci. Data*, 14, 2865–2882,
867 <https://doi.org/10.5194/essd-14-2865-2022>, 2022.

868

869 Maussion, F., Butenko, A., Champollion, N., Dusch, M., Eis, J., Fourteau, K., et al. The open global glacier
870 model (OGGM) v1.1. *Geoscientific Model. Develop.* 12, 909–931. <https://doi.org/10.5194/gmd-12-909-2019>,
871 2019.

872

873 Meier, W.J.-H., Grieflinger, J., Hochreuther, P. and Braun, M.H. An Updated Multi-Temporal Glacier Inventory
874 for the Patagonian Andes With Changes Between the Little Ice Age and 2016, *Front. Earth Sci.*, 6:62.
875 <https://doi.org/10.3389/feart.2018.00062>, 2018.

876

877 Millan, R., Mougnot, J., Rabatel, A. et al. Ice velocity and thickness of the world’s glaciers. *Nat. Geosci.* 15,
878 124–129. <https://doi.org/10.1038/s41561-021-00885-z>, 2022.

879

880 NASA JPL. NASADEM Merged DEM Global 1 arc second V001 [Data set]. NASA EOSDIS Land Processes
881 DAAC. https://doi.org/10.5067/MEaSURES/NASADEM/NASADEM_HGT.001, 2020.

882

883 Rabassa, J. El cambio climático global en la Patagonia desde el viaje de Charles Darwin hasta nuestros días.

884 Revista de la Asociación Geológica Argentina, 67(1), 139-156, 2010.

885

886 Rabatel, A., Bermejo, A., Loarte, E., Soruco, A., Gomez, J., Leonardini, G., Vincent, C., and Sicart, J. E.:

887 Relationship between snowline altitude, equilibrium-line altitude and mass balance on outer tropical glaciers:

888 Glaciar Zongo – Bolivia, 16° S and Glaciar Artesonraju – Peru, 9° S, J. Glaciol., 58, 1027–1036,

889 <https://doi.org/10.3189/2012JoG12J027>, 2012.

890

891 Rabatel, A., Castebrunet, H., Favier, V., Nicholson, L., and Kinnard, C. Glacier Changes in the Pascua-Lama

892 Region, Chilean Andes (29° S): Recent Mass Balance and 50 Yr Surface Area Variations. The Cryosphere 5 (4),

893 1029–1041. <https://doi.org/10.5194/tc-5-1029-2011>, 2011.

894

895 Rabatel, A., Francou, B., Soruco, A., Gomez, J., Cáceres, B., Ceballos, J. L., et al. Current State of Glaciers in

896 the Tropical Andes: A Multi-century Perspective on Glacier Evolution and Climate Change. The Cryosphere 7,

897 81–102. <https://doi.org/10.5194/tc-7-81-2013>, 2013.

898

899 Ragetli, S., and Pellicciotti, F. Calibration of a Physically Based, Spatially Distributed Hydrological Model in a

900 Glacierized basin: On the Use of Knowledge from Glaciometeorological Processes to Constrain Model

901 Parameters. Water Resour. Res. 48 (3), 1–20. <https://doi.org/10.1029/2011WR010559>, 2012.

902

903 RGI Consortium. Randolph Glacier Inventory - A Dataset of Global Glacier Outlines, Version 6. Boulder,

904 Colorado USA. NSIDC: National Snow and Ice Data Center, <https://doi.org/10.7265/4m1f-gd79>, 2017.

905

906 Rivera, A. Mass balance investigations at Glaciar Chico, Southern Patagonia Icefield, Chile. PhD thesis,

907 University of Bristol, UK, 303 pp, 2004.

908

909 Robson, B. A., MacDonell, S., Ayala, Á., Bolch, T., Nielsen, P. R., and Vivero, S. Glacier and rock glacier

910 changes since the 1950s in the La Laguna catchment, Chile, The Cryosphere, 16, 647–665,

911 <https://doi.org/10.5194/tc-16-647-2022>, 2022.

912

913 Ruiz, L., Berthier, E., Viale, M., Pitte, P., and Masiokas, M. H. Recent geodetic mass balance of Monte Tronador

914 glaciers, northern Patagonian Andes, The Cryosphere, 11, 619–634, <https://doi.org/10.5194/tc-11-619-2017>,

915 2017.

916

917 Rounce, D.R., Khurana, T., Short, M.B., Hock, R., Shean, D.E., Brinkerhoff, D.J. Quantifying parameter

918 uncertainty in a large-scale glacier evolution model using Bayesian inference: application to High Mountain

919 Asia. Journal of Glaciology, 66(256):175-187, <https://doi.org/10.1017/jog.2019.91>, 2020.

920

921 Schaefer M., Rodriguez J., Scheiter M., and Casassa, G. Climate and surface mass balance of Mocho Glacier,
922 Chilean Lake District, 40°S. *Journal of Glaciology*, 63(238), 218-228, <https://doi.org/10.1017/jog.2016.129>,
923 2017.
924

925 Schuster. L., Rounce, D.R., Maussion, F. Glacier projections sensitivity to temperature-index model choices and
926 calibration strategies. *Annals of Glaciology*, 1-16, <https://doi.org/10.1017/aog.2023.57>, 2023
927

928 Seehaus, T., Malz, P., Sommer, C., Lippl, S., Cochachin, A., and Braun, M. Changes of the tropical glaciers
929 throughout Peru between 2000 and 2016 – mass balance and area fluctuations, *The Cryosphere*, 13, 2537–2556,
930 <https://doi.org/10.5194/tc-13-2537-2019>, 2019.
931

932 Seehaus, T., Malz, P., Sommer, C., Soruco, A., Rabatel, A., and Braun, M. Mass balance and area changes of
933 glaciers in the Cordillera Real and Tres Cruces, Bolivia, between 2000 and 2016. *J. Glaciol*, 66(255), 124-136.
934 <https://doi.org/10.1017/jog.2019.94>, 2020.
935

936 SENAMHI, datos hidrometeorológicos de Perú [data set],
937 <https://www.senamhi.gob.pe/?p=descarga-datos-hidrometeorologicos>, 2022.
938

939 Shaw, T. E., Caro, A., Mendoza, P., Ayala, Á., Pellicciotti, F., Gascoin, S., et al. The Utility of Optical Satellite
940 Winter Snow Depths for Initializing a Glacio-Hydrological Model of a High-Elevation, Andean Catchment.
941 *Water Resour. Res.* 56 (8), 1–19. <https://doi.org/10.1029/2020WR027188>, 2020.
942

943 Sicart, J. E., Wagon, P., and Ribstein, P. Atmospheric controls of heat balance of Zongo Glacier (16°S. Bolivia).
944 *J. Geophys. Res.* 110:D12106. <https://doi.org/10.1029/2004JD005732>, 2005.
945

946 Sicart, J. E., P. Ribstein, B. Francou, B. Pouyaud, and T. Condom. Glacier mass balance of tropical Zongo
947 Glacier, Bolivia, comparing hydrological and glaciological methods, *Global Planet. Change*, 59(1), 27– 36,
948 <https://doi.org/10.1016/j.gloplacha.2006.11.024>, 2007.
949

950 Sicart, J. E., R. Hock, and D. Six. Glacier melt, air temperature, and energy balance in different climates: The
951 Bolivian Tropics, the French Alps, and northern Sweden, *J. Geophys. Res.*, 113, D24113,
952 <https://doi.org/10.1029/2008JD010406>, 2008.
953

954 Stuefer, M. Investigations on Mass Balance and Dynamics of Moreno Glacier Based on Field Measurements and
955 Satellite Imagery. Ph.D. Dissertation, University of Innsbruck, Innsbruck, 1999.
956

957 Stuefer, M., Rott, H. and Skvarca, P. Glaciar Perito Moreno, Patagonia: climate sensitivities and glacier
958 characteristics preceding the 2003/04 and 2005/06 damming events. *J. Glaciol.*, 53 (180), 3–16.
959 <https://doi.org/10.3189/172756507781833848>, 2007.
960

961 Soruco, A., Vincent, C., Rabatel, A., Francou, B., Thibert, E., Sicart, J. E., et al. Contribution of Glacier Runoff
962 to Water Resources of La Paz City, Bolivia (16° S). *Ann. Glaciol.* 56 (70), 147–154.
963 <https://doi.org/10.3189/2015AoG70A001>, 2015.

964

965 Takeuchi, Y., Naruse R. and Satow K. Characteristics of heat balance and ablation on Moreno and Tyndall
966 glaciers, Patagonia, in the summer 1993/94. *Bulletin of Glacier Research*, 13, 45-56, 1995.

967

968 WGMS. Global Glacier Change Bulletin No. 4 (2018-2019). Michael Zemp, Samuel U. Nussbaumer, Isabelle
969 Gärtner-Roer, Jacqueline Bannwart, Frank Paul, and Martin Hoelzle (eds.), ISC (WDS) / IUGG (IACS) / UNEP /
970 UNESCO / WMO, World Glacier Monitoring Service, Zurich, Switzerland, 278 pp. Based on database version
971 <https://doi.org/10.5904/wgms-fog-2021-05>, 2021.

972

973 Zhang, G.Q., Bolch, T., Yao, T.D., Rounce, D.R., Chen, W.F., Veh, G., King, O., Allen, S.K., Wang, M.M.,
974 Wang, W.C. Underestimated mass loss from lake-terminating glaciers in the greater Himalaya. *Nat. Geosci.* 16,
975 333–338. <https://doi.org/10.1038/s41561-023-01150-1>, 2023.

976

977 Zimmer, A., Meneses, R. I., Rabatel, A., Soruco, A., Dangles, O., and Anthelme, F. Time Lag between Glacial
978 Retreat and Upward Migration Alters Tropical alpine Communities. *Perspect. Plant Ecol. Evol. Syst.* 30, 89–102.
979 <https://doi.org/10.1016/j.ppees.2017.05.003>, 2018.